Nanoscale Advances



REVIEW

View Article Online
View Journal | View Issue



Cite this: Nanoscale Adv., 2024, 6, 1331

Nanocrystals as performance-boosting materials for solar cells

Boping Yang, (10 ** Junjie Cang, b Zhiling Lia and Jian Chen*c

Nanocrystals (NCs) have been widely studied owing to their distinctive properties and promising application in new-generation photoelectric devices. In photovoltaic devices, semiconductor NCs can act as efficient light harvesters for high-performance solar cells. Besides light absorption, NCs have shown great significance as functional layers for charge (hole and electron) transport and interface modification to improve the power conversion efficiency and stability of solar cells. NC-based functional layers can boost hole/electron transport ability, adjust energy level alignment between a light absorbing layer and charge transport layer, broaden the absorption range of an active layer, enhance intrinsic stability, and reduce fabrication cost. In this review, recent advances in NCs as a hole transport layer, electron transport layer, and interfacial layer are discussed. Additionally, NC additives to improve the performance of solar cells are demonstrated. Finally, a summary and future prospects of NC-based functional materials in solar cells are presented, addressing their limitations and suggesting potential solutions.

Received 29th November 2023 Accepted 31st January 2024

DOI: 10.1039/d3na01063e

rsc.li/nanoscale-advances

1. Introduction

Nanocrystals (NCs), sometimes termed as quantum dots (QDs) or nanoparticles (NPs), with a size less than 100 nm, are popular worldwide and have been paid extensive attention owing to their outstanding photoelectric properties. In the energy field, photovoltaic devices based on semiconductor NCs are among the most potential systems with high power conversion efficiency (PCE), good stability, low cost, facile fabrication, and other advantages. 1-16 In recent years, NCs have been widely used as light harvesting layers in high-performance solar cells. Semiconducting NCs such as PbX (X = S, Se, and Te), CdSe, and CuInS₂ have been suggested as excellent light harvesters in third-generation solar cells. 11,14,15,17-22 Additionally, perovskite NCs are also good alternatives for light harvesting in solar cells. 12-14,16,23-28 Besides active layers (light harvesting layers), functional layers based on NCs, mainly including hole transport layers (HTLs),29-99 electron transport layers (ETLs)100-173 and interfacial functional layers (IFLs), 174-221 are of great importance in solar cells. Notably, NC additives also boost the performance of solar cells through defect passivation, plasmonic effect, solar concentration, light up-conversion and down-conversion/ shifting, light scattering and reflection, and heat sinks.²²²⁻²⁵⁸

To efficiently transport charge in solar cells, HTLs and ETLs must have suitable energy levels matching the active layers such

as dyes, Si, Pb-based light harvesting layers, and perovskite films. For example, to fabricate high-performance perovskite solar cells (PSCs), the work function of HTLs and ETLs should have hole and electron transport layers aligned with the valence band edge and conduction band edge of a perovskite. As is well known, the energy levels of NCs can be easily controlled and adjusted by changing their sizes, ligands, and dopants during their synthesis process, which is favourable to satisfy the energy alignment. Meanwhile, the easily-accomplished modifications in NCs mentioned above also favour high mobility to allow carrier transport and form a more effective current circulation path. Furthermore, the transmittance of HTL or ETL based on NCs can be improved during synthesis processes, which leads to less light loss and thus, higher performance of solar cells. Consequently, NCs are a good choice as HTLs and ETLs for efficient solar cells and have gained much attention.

Some researchers found that inserting different IFLs in solar cells could promote the power conversion efficiency (PCE) and stability of the devices. Good IFL can modulate the formation of adjacent layers (especially the perovskite layer in PSCs), optimize energy alignment, and impede charge recombination. As multi-functional IFL, NCs have been extensively investigated due to their compatible properties, such as appropriate morphology for compact, smooth films, gradual energy level to transfer carriers, and self-stability to protect the devices.

Besides acting as a separate functional layer in efficient solar cells, NCs have also been used as additives to improve active layer quality, accelerate carrier transfer, convert infrared or ultraviolet light to visible light, scatter and reflect light, sink heat, and other functions.^{222–258} The addition of NCs could enlarge the grain size of perovskite film, reduce the

^aCollege of Science, Guizhou Institute of Technology, Guiyang, 550003, China. E-mail: bpyang023@163.com

^bSchool of Electrical Engineering, Yancheng Institute of Technology, Yancheng, 224051, China

College of Artificial Intelligence and Electrical Engineering, Guizhou Institute of Technology, Guiyang, 550003, China. E-mail: cjycit@163.com

Nanoscale Advances Review

recombination, enhance charge extraction, improve the charge mobility, broaden the spectral response range, and so on.

In this review, functional materials based on NCs for highperformance solar cells are summarized. NCs as HTL, ETL, IFL, and additives for NC-light-harvestor solar cells (NC-LHSCs), PSCs, organic solar cells (OSCs), Si solar cells, and dye-sensitized solar cells (DSSCs) are successively analyzed. In Section 2, NCs as charge transport layers are analyzed in detail. This can provide a deep understanding of the extensive application of NCs in solar cells. As an important functional layer, IFL based on NCs is summarized in the next section. Section 4 describes NCs as efficient additives in different functional layers due to their small sizes and excellent photoelectric properties. Finally, we discuss the existing challenges of NCs for boosting the performance of solar cells and provide some feasible suggestions on these issues, expecting to improve the performance of solar cells based on NCs.

Nanocrystals as charge transport layers

In this section, we focus on NCs-based charge transport layers for solar cells, mainly including top/bottom HTL and ETL in n-ip and p-i-n solar cells.

2.1 Nanocrystals as HTL

As known to us, solar cells work as follows: absorption of sun light, generation and separation of hole-electron pairs, transport of holes through HTL and electrons through ETL, and current produced by the flow of electrons through external circuits. Solar cells using NCs as HTL are not exceptional, and the typical structures of solar cells based on NC HTL are shown in Fig. 1. According to the position of HTL, we call HTL between the ITO/FTO and active layer as bottom HTL while the HTL between metal electrode and active layer as top HTL.

2.1.1 Recent NC HTL. Semiconductor NCs have shown great potential in photoelectronic devices due to their excellent properties. The advances of NC HTLs for solar cells are listed in Table 1, including the size of NCs, device structure, PCE, and stability of solar cells.

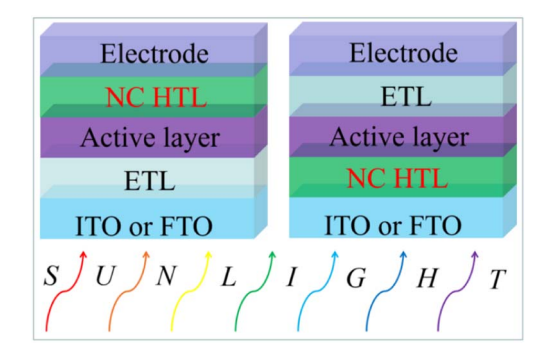


Fig. 1 Typical structure of solar cells based on top (left) and bottom (right) NC HTLs.

Lead chalcogenide NCs, especially PbS, have been massively used as efficient top HTL in NC-LHSCs.29-56 Additionally, other metal chalcogenide NCs are also excellent choices as top HTL for high-performance perovskite solar cells (PSCs), mainly containing CuInS₂/ZnS (core/shell),⁵⁷ CdZnSe@ZnSe,⁵⁸ Cu₂-ZnSnS₄/Se₄,⁵⁹ SnS,⁶⁰ CuInSe₂,⁶¹ Ag-In-Ga-S,⁶² Cu₁₂Sb₄S₁₃,⁶³ Cu₂SnS₃,64 CuGaS,65 and CuInS₂.66 Metal oxide NCs of NiO have shown potential for hole transport on top of the light harvesting layer in PSCs and Si solar cells. 67-69 Besides NiO, some other metal oxide NCs such as MoO₂, 70 Co₃O₄, 71 Cu₂O, 72 CuCrO₂, 73 CuGaO₂,⁷⁴ and CsPbI₃ (ref. 75) have been used as efficient top HTL for PSCs due to their excellent properties. It can be noticed that when PbS NCs are used as top HTL in solar cells, the light harvesting layers are mostly based on the PbS/Se family. There are not many perovskite used as light harvest materials when PbS/Se is used as top HTL. Only MAPbI₃ was applied in 2015, and 7.88% PCE was gained.29 We suppose this is because the PbS NCs with long carbon chains or 1,2-ethanedithiol are not good at charge transport. If high-temperature annealing is adopted to enhance the conductivity of PbS, the perovskite underneath will be destroyed. This encourages us to regulate the synthesis or modification of NCs with less or even no charge transfer inhibition capture and improve their electronic properties.

Similar to top HTL, NCs can also be applied as bottom HTL for high-performance solar cells. NCs of PbS,76 Cu2ZnSnS4,77,78 NiO_x and its doped derivatives, 79-91 CuO, 92 and ternary oxides of CuCrO₂, 93,94 CuGaO₂, 95 NiCo₂O₄, 96,97 ZnCoO₄, 98 and doped ternary oxide In:CuCrO2 (ref. 99) have offered excellent hole transport ability in PSCs and PTB7-Th-based organic solar cells (OSCs).

Ever since demonstrated as efficient HTL by Luther et al. in 2008,²⁴⁸ PbS NCs with a 1,2-ethanethiol (EDT) ligand (named as PbS-EDT or EDT-PbS) have been massively applied for hole transport in solar cells. From the established NC HTLs listed in Table 1, we can find some regular patterns: (i) as top HTL, EDTlinked sulphides were mainly used in NC-LHSCs but were not popular in PSCs. This is because EDT will strongly attack the perovskite materials in the n-i-p device and decrease the device performance.61 (ii) As bottom HTL, oxides are widely used and sulphides are rare. We speculate that it is (iii) NiOx with high hole transport quality mostly used to transport holes in PSCs.

The previous light harvesting NC layers are mainly based on the Pb-based chalcogenide family or their mixture. NC-LHSCs using NCs as HTL have gained high PCE above 13%,45,50 but this is significantly lower than that of the theoretical value.¹¹ Some strategies were also adopted to modify the lightharvesting NCs, which is not the keynote in this review. The current relatively low PCE of NC-LHSCs may be on account of non-radiative recombination resulting from the high density of surface traps due to some intrinsic properties of NCs, such as high surface-to-volume ratios. Using NC top HTL, the PCE value can be improved. Some oxides, for instance, NiO, Ti-doped MoO₂, Co₃O₄, Cu₂O, CuCrO₂, and CuGaO₂, have acted as excellent top HTL in high-performance PSCs. As shown in Fig. 2a, SnS NCs prepared by the one-pot hot-injection method utilized as top HTL in efficient and stable

Table 1 Recent advances in selected NC HTLs for solar cells (EDT = 1,2-ethanedithiol, relative humidity = RH)

	NC	Active layer	PCE (%)	Long-term stability	Ref
Тор НТL	PbS-EDT	CH ₃ NH ₃ PbI ₃	7.88	8% decay after 2 days	29
		PbS	11.6	Null	30
			10.4	100%, after 103 days in the dark under ambient conditions	32
			9.44	\sim 100%, after 4 months in ambient air	33
			13.2	Null	37
			10.4	①96%, after baking on a hotplate in air for 120 min; ②97%, after 60 min oxygen plasma treatment	38
			13.3	Null	39
			10.5	Null	40
			13.0	Null	41
		PbS-PbI ₂	$\textbf{11.2} \pm \textbf{0.22}$	Nearly no drop of PCE after 180 h under continuous heating at 85 °C in ambient air	44
			11.29	>90, after 600 h under ambient condition	45
		PbS:F	12.7	Null	46
		PbX ₂ -PbS	8.16	Null	47
			10.35	Null	48
			10.6	Null	49
		PbS-PbX ₂ -KI ₃	12.1	94%, after 20 h continuous operation in air	50
		PbSe-PbS	1.24 (infrared PCE)	~95%, after 25 days in air	51
		PbSe-PbI ₂	10.4	90%, after 30 days in ambient condition	51
		CsMAFA-PbS	11.3	96%, after 1200 h shelf storage	53
		MAPbI ₃ –PbS	9.5	95%, after 2 months in ambient environment	54
		Sb_2Se_3	6.5 (certified)	Null	55
		KPbS	12.6	83%, after 300 h under continuous operation at MPP in ambient air	56
	CuInS ₂ /ZnS core/shell	$MAPbI_3$	8.38	Null	57
	CdZnSe@ZnSe	CdZnSe@ZnSe	8.65	Null	58
	Cu ₂ ZnSnSe ₄ Cu ₂ ZnSnS ₄	$MAPbI_3$	9.72 10.72	Null	59
	SnS	$(CsPbI_3)_{0.05}(FAPbI_3)_{0.79}$ $(MAPbI_3)_{0.16}$	13.7	①99%, after 1000 h storage in air; ②75%, after 500 h under continuous 1 sun	60
		$(PbI_3)_{0.03}$		illumination in a N ₂ atmosphere at 25 °C	
	CuInSe ₂	MAFAPbClBrI	12.8	78%, after 96 h in air	61
	Ag-In-Ga-S	CsPbBr ₃	8.46	96.1%, after 240 h in air	62
	$Cu_{12}Sb_4S_{13}$	CsPbI ₃	10.02	94%, after storage in ambient air for 360 h	63
	Cu_2SnS_3	$Cs_{0.05}(MA_{0.17}-FA_{0.83})_{0.95}Pb(I_{0.83}Br_{0.17})_3$	13.01	90%, after 1200 h in an ambient atmosphere	64
	CuGaS	$(FAPBI_3)_{1-x}(MAPbBr_3)_x$	17.56	81%, aging for 30 days	65
	$CuInS_2$	$(FAPBI_3)_{1-x}(MAPbBr_3)_x$	18.81	91%, aging for 30 days	66
	NiO	$MAPbI_3$	6.2	Null	67
		MAPbI ₃ NCs	10.89	Null	68
	Ti-doped MoO ₂	$MAPbI_3$	15.8	\sim 95%, after 15 days with 50–70% RH	70
	$\mathrm{Co_3O_4}$	$MAPbI_3$	13.27	Up to 2500 hours under ambient conditions	71
	Cu_2O	$Cs_{0.05}FA_{0.81}MA_{0.14}PbI_{2.55}Br_{0.45}$	18.9	80%, after 30 days in air with \sim 30% RH	72
	CuCrO ₂	$Cs_{0.05}(MA_{0.15}FA_{0.85})_{0.95}$ $Pb(I_{0.85}Br_{0.15})_3$	16.68	88%, after 500 h at the MPP under one sun and a N_2 atmosphere	73
	CuGaO ₂	$MAPbI_3$	18.51	>85%, after 30 days at 25 °C with 30–55% humidity without encapsulation	74
	$CsPbI_3$	$MAPbI_3$	17.0	Null	75

Table 1 (Contd.)

	NC	Active layer	PCE (%)	Long-term stability	Ref.
Bottom	PbS	$MAPbI_3$	7.5	Null	76
HTL	Cu_2ZnSnS_4	$MAPbI_3$	15.4	Null	77
			6.02	87%, after 43 days in N ₂ atmosphere	78
	Ni-NiO core-shell	РЗНТ	0.86	Null	79
	NiO_x	$Cs_{0.08}(MA_{0.17}FA_{0.83})_{0.92}$ Pb $(I_{0.83}Br_{0.17})_3$	12.8	Null	81
		$MAPbI_3$	16.1	90%, after 60 days in air at RT	84
		$Cs_{0.05}(MA_{0.17}FA_{0.83})_{0.95}$ Pb $(I_{0.9}Br_{0.1})_3$	18.6	>80%, after 1000 h	85
		$MAPbI_3$	17.60	93%, after 30 days	86
			1.02 cm ² : 18.49 (rigid) and 15.89 (flexible)	90%, after 500 h in the thermal aging test (85 °C, 85% RH)	87
	Cu:NiO _r		15.01	86%, after 1 month in an ambient	88
	0310.101		(flexible, >1 cm ²)	environment at 25 °C with about 40% humidity	
			18.3	Null	89
	(Li,Cu):NiO _x	$MAPbI_{3-x}Cl_{x}$	20.80	95%, after 60 days of storage	90
	NiO_x	$CsPbI_xBr_{3-x}$	16.1	85%, after 350 h light soaking	91
	CuO	$MAPbI_3$	15.3	Null	92
	CuCrO ₂		19.0	\sim 90, after 30 days in an Ar-filled dry glove box and continuously irradiated by a UV optical fiber with 5 mW cm ⁻²	94
	$CuGaO_2$		15.6	Null	95
	$NiCo_2O_4$	$MAPbI_{3-x}Cl_x$	18.23	\sim 90%, after 500 h illumination at AM 1.5G	96
	$ZnCo_2O_4$	PTB7-Th:PC ₇₁ BM	9.37	>60%, after 60 h in ambient environment with 50% RH without capsulation	98
		$MAPbI_{3-x}Cl_x$	18.14	>60%, after 110 h in ambient environment with capsulation and under continuous 1 sun illumination soaking	
	In:CuCrO ₂	$Cs_{0.05}(MA_{0.15}FA_{0.85})_{0.95}$ $Pb(I_{0.85}Br_{0.15})_3$	20.54	\sim 90%, after 800 h of continuous radiation in glovebox	99

(CsPbI₃)_{0.05}(FAPbI₃)_{0.79}(MAPbI₃)_{0.16} PSCs. The high PCE mainly resulted from good surface coverage and an excellent hole extraction ability demonstrated by Nyquist plots. Additionally, SnS-based PSC presented better air stability than the 2,2′,7,7′-tetrakis[N,N-di(4-methoxyphenyl)amino]-9,9′-spirobifluorene (spiro-OMeTAD)-based device. Surface-modified Cu₂O NCs boosted the efficiency of PSC to 18.9% with distinctly better stability than the reference device based on spiro-OMeTAD.⁶¹ One important reason is the difference in hydrophobicities illustrated by water contact angles in Fig. 2b. Ternary oxide CuGaO₂NCs with promising photoelectronic properties boosted the n-i-p PSCs with higher PCE and stability than spiro-OMeTAD (Fig. 2c).⁷⁵

In n-i-p type solar cells, NiO_X and its doped family oxide NCs are the most popular NC HTLs because of their facile synthesis and outstanding photoelectronic properties. 86,101 Meanwhile, sulphides of PbS and $\mathrm{Cu}_2\mathrm{ZnSnS}_4$ together with multi basic oxides of CuCrO_2 , CuGaO_2 , $\mathrm{NiCo}_2\mathrm{O}_4$, $\mathrm{ZnCo}_2\mathrm{O}_4$, and $\mathrm{In:CuCrO}_2$ are valuable substitutes for NiO_X family. Ligand-free NiO_X NCs in ethanol (E-NiO_X) are spin-coated onto a substrate to form a smooth and compact NiO_X film that has good hole extraction capability. As seen in Fig. 3a, this E-NiO_X bottom HTL can be

used both in rigid and flexible PSC, producing high PCE and stability. Similar to top HTL, ternary oxide NCs like CuCrO₂ were also utilized as bottom HTL for high-performance solar cells. The low-temperature solution-processed CuCrO₂ NCs provide suitable electronic structure, charge carrier transport properties, and greater UV light-harvesting, demonstrating its potential as an efficient HTL for highly efficient and photostable n-i-p PSCs (Fig. 3b).

2.1.2 Advantages of NC HTL. One important inherent advantage of semiconductor NCs is their bandgap variation along with modification. The conduction band, valence band, and Fermi level of PbS NCs can be modified by changing surface ligands (Fig. 4), thus enhancing the performance of solar cells.252 Fig. 4 shows that the energy level of PbS NCs is easily changed in a large range by different ligands, facilitating energy matching with the light-harvesting layer and other functional layers. Compared with mostly used organic HTLs of spiro-OMeTAD, poly(3,4-ethylenedioxythiophene):poly(styrenesulfonate) (PEDOT:PSS) and poly[bis(4-phenyl)(2,4,6trimethylphenyl)amine] (PTAA), inorganic NCs show higher stability with good hole transport ability, suggesting great potential for boosting solar cell performance. Equally

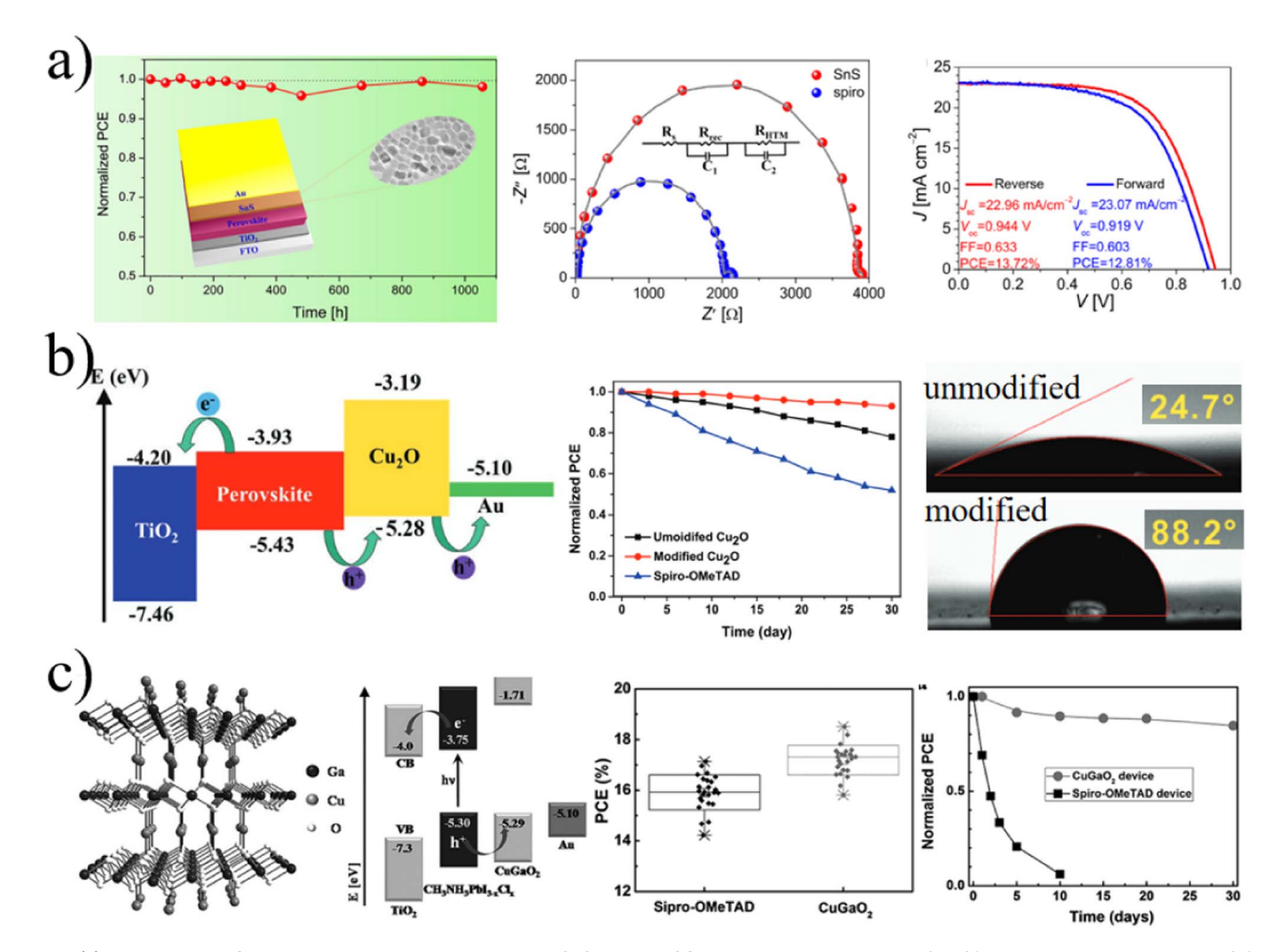


Fig. 2 (a) Evolution of PCE over time of the unencapsulated SnS-based PSCs in the ambient air of \sim 30–50% humidity, Nyquist plots at 0.9 V forward bias measured in the dark, forward, and reverse J-V curves of champion PSCs based on SnS. (b) Schematic view of PSC configuration, device performance durability of PSCs based on different HTLs in ambient air for 30 days, and water contact angles of unmodified and modified Cu₂O. (c) Schematic illustration of the crystal structure of CuGaO₂, device architecture of a regular PSC based on CuGaO₂, standard deviations of PCEs to evaluate reproducibility by statistics of 50 devices based on CuGaO₂ and spiro-OMeTAD. (a) Adapted with permission. ⁵¹ Copyright 2019, American Chemical Society. (b) Adapted with permission. ⁷³ Copyright 2019, Wiley-VCH. (c) Adapted with permission. ⁷⁵ Copyright 2017, Wiley-VCH.

important, facile synthesis and low cost would be helpful for the commercialization of new-generation solar cells.

2.1.3 Potential NC HTL. To further develop more strategies for fabricating high-performance solar cells and boost the device PCE and stability, we should find more potential NCs for efficient hole transport in solar cells. According to the previous reports and our understanding, excellent NC HTLs should satisfy the following requirements: (i) matched energy level alignments with other functional layers; (ii) high hole mobility and conductivity; (iii) enhancing the quality of adjacent layers; (iv) intrinsic resistance to heat, light and water; (v) convenient fabrication with low cost; and (vi) high transmittance for bottom HTL and reflectivity for top HTL. NCs have many good properties such as easily-controlled energy level, excellent spreading and filling ability due to their small sizes, stable intrinsic structure, skilled synthesis process, and variant surface ligand. Considering the above rules and the advantages

of NCs, besides the existing NC HTLs, some other p-type sulphide and oxide NCs have huge potential for efficient and stable solar cells. Additionally, semiconductor NCs with enhanced hole-transporting ability by p-type doping are also good alternatives.

2.2 Nanocrystals as ETL

2.2.1 Recent advances of NC ETL. As important as HTL, ETL is also of great significance for high-performance solar cells to transport electrons and block holes, and it acts as well as a trap passivating layer and water/oxygen preventing layer. The typical structure of solar cells based on NC ETL is shown in Fig. 5.

ZnO is good at electron transport in photoelectrical devices due to excellent properties such as bandgap (3.3 eV), low cost, high electron mobility ($\sim 10^{-5}-10^2~{\rm cm^2~V^{-1}~s^{-1}}$), and matching energy levels. ^{100,101} ZnO NCs with different sizes have been used

Nanoscale Advances

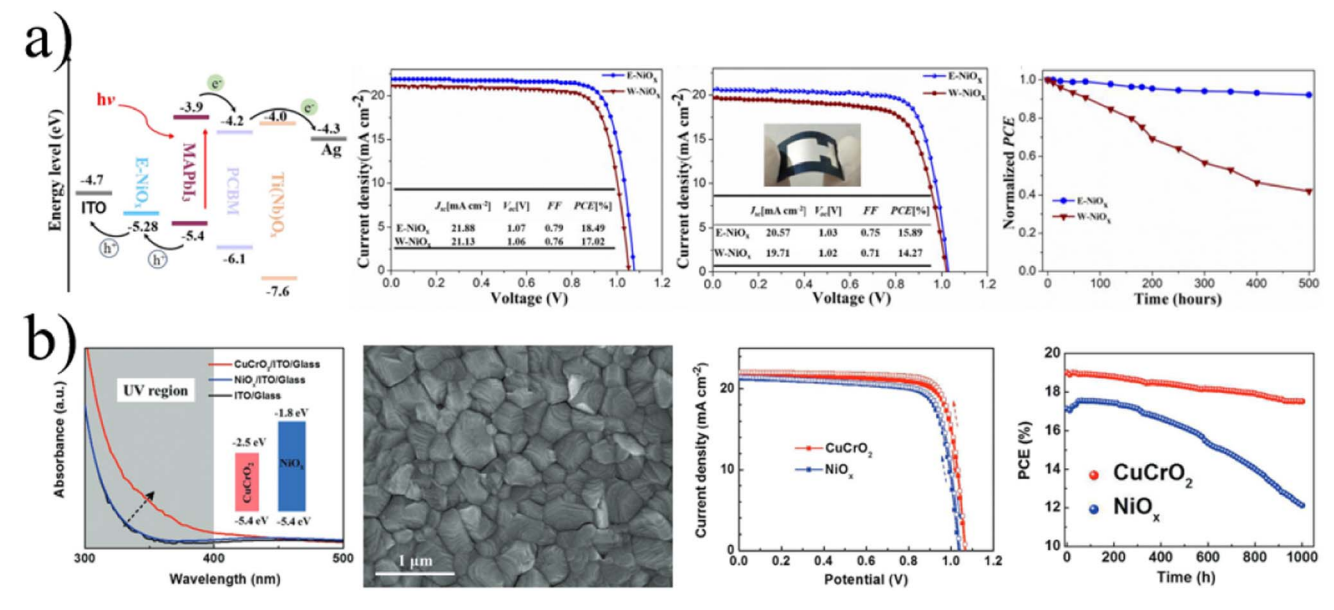


Fig. 3 (a) Energy level diagram of the materials used in the device, J-V curves of rigid and flexible PSCs, normalized PCE. (b) UV-vis spectra of the CuCrO₂ and NiO_x layer with optimum thickness with energy level in the inset. Adapted with permission.^{87,94} Copyright 2018, Wiley-VCH.

as efficient top ETL in NC-LHSCs, OSCs, and PSCs. 43,84,85,91,101-108 TiO2 and SnO2NCs are as popular as ZnO for electron transport due to their outstanding photoelectronic properties of high mobility and conductivity.²⁵⁰ Certainly, these oxide NCs can be modified by doping, ligand changing, and other strategies. Tetrabutylammonium hydroxide (TBAOH)-capped metal oxide NCs for SnO₂ also extend to TiO₂, ITO and CeO₂NCs as top ETL for PSCs.108 TiO2NCs have always been as the top ETL for PSCs. 109-111 CeOx, 112 In2O3 and its Sn doped derivative formed bilayer ETL,113 and CdSe114 were also used for high-performance n-i-p PSCs. As efficient bottom ETL, modified TiO₂ by Sn, Al, Co, Cu, and N doping and N, F and S co-doped graphene NCs were widely used in dye-sensitized solar cells (DSSCs) based on N719 and N3 ({cis-Ru(H₂dcbpy)₂(NCS)₂, H₂dcbpy = 4,4'-dicarboxy-2,2'-bipyridyl }).115-120 Additionally, TiO2, CdS NCs-modified TiO₂, and Nb-doped TiO₂NCs were applied for electron transport in PSCs with high PCE and stability. 121-123 Meanwhile, TiO2NCs have been widely applied in n-i-p solar cells using chalcogenide NC as light harvesters, such as CdSe, CdS, and PbS. 124-130 Similarly, ZnO NCs were used as ETL for n-i-p PbS-

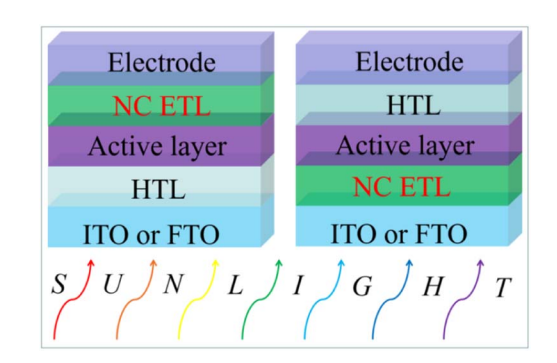


Fig. 5 Structure of solar cells based on top (left) and bottom (right) NC ETLs.

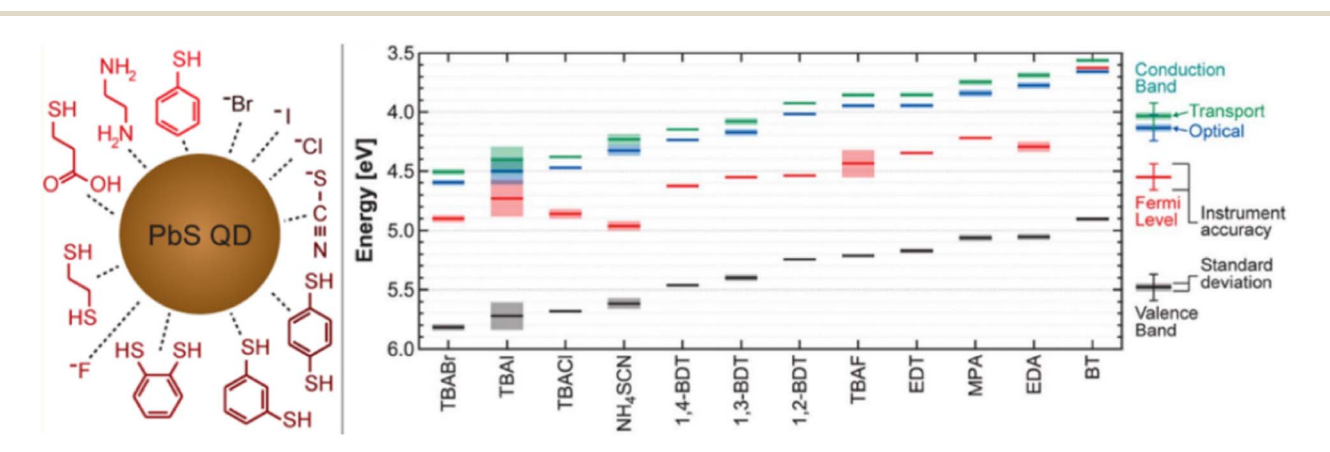


Fig. 4 Energy band position of PbS NC films for different surface ligands. Adapted with permission.²⁴⁹ Copyright 2014, American Chemical Society.

Table 2 Recent advances in NC ETLs (bathocuproine = BCP)

	NC	Active layer	PCE (%)	Long-term stability	Re
Top ETL	ZnO	PbS-PbX ₂	10.35	Null	43
		PCDTBT:PC ₆₁ BM	2.66	Null	10
		$CsPbI_3NCs$	13.1	80%, after 40 h under 25 °C with 30–40% RH	10
		$MAPbI_3$	17.2	66%, after 120 days stored in air	10
		$MAPbI_3$	16.1	90% after 60 days in air at RT	84
		$Cs_{0.05}(MA_{0.17}FA_{0.83})_{0.95}Pb(I_{0.9}Br_{0.1})_3$	18.6	>80% after 1000 h	85
		$CsPbI_xBr_{3-x}$	16.1	85%, after 350 h light soaking	91
	Ag modified BCP:ZnO	$MAPbI_3$	15.5	Null	10
	In:ZnO	$MAPbI_3$	16.2	85% after 460 h of light soaking	10
	TBAOH-SnO ₂	$MAPbI_3$	18.77	90% after aging at 45 °C for 240 h, followed by 65 °C for 240 h and 85 °C for 240 h	10
	TiO_2	$Cs_{0.05}(MA_{0.15}FA_{0.85})_{0.95}Pb(I_{0.85}Br_{0.15})_3$	20.5	\sim 90% after 350 h MPP tracking test	10
	Carbide-TiO ₂	CsPbI ₂ Br	14.8	①>94%, after 1000 h at 85 °C in dark under N_2 ; ②>90%,	11
				after 1000 h at 60 °C under continuous illumination	
	CeO_x	$MAPbI_3$	16.7	100%, after 200 h in air with 30% RH	11
	Sn:In ₂ O ₃ /In ₂ O ₃ (bilayer)	$Cs_{0.05}(MA_{0.15}FA_{0.85})_{0.95}Pb(I_{0.85}Br_{0.15})_3$	20.65	⊕91.9% after 69 days under 85 °C;@91.8% after 2000 h, 12 h continuous 1 sun illumination and then 12 h	11
				interval in the dark	
	CdSe	$MAPbI_3$	15.1	Null	1:
ottom ETL	Sn:TiO ₂	N719	6.24	Null	1
JUIN ETL	Al:TiO ₂	11/19	4.27	Null	1
	Co:TiO ₂		4.27	Null	1
	-	N3/electrolyte	6.51	Null	1
	Ti _{0.94} Cu _{0.06} O ₂ TiO ₂ modified by N, F and S, co-doped graphene NCs	N719	11.7	\sim 85.5, after one month	1
	TiO ₂	Cs-FA-MA mixed cation perovskite	19.03	84%, after 30 days	1
	CdS NCs-modified TiO ₂	MAPbI ₃	8.16	Null	1
	Nb-doped TiO ₂	-	18.97	Null	1
	TiO ₂	$Cs_{0.05}(MA_{0.15}FA_{0.85})_{0.95}Pb(I_{0.85}Br_{0.15})_3$ CdS	4.59	Null	1
	Cu_2O doped TiO_2	CdSe/CdS/ZnS/electrolyte	3.01	Null	1
	TiO ₂	Mn-CdSe	3.55	Null	1
	TiO_2	CdSe/ZnS/SiO ₂ /Cu ₂ S	4.00	Null	1
	Cl@ZnO	PbS	11.6	Null	3
	ZnO	PbX ₂ -PbS	9.5	95%, after 2 months in ambient environment	3
	MgZnO	PbS	10.4	100%, after 103 days in the dark under ambient conditions	3
	ZnO	Lead halide-PbS	12.7	Null	4
	ZnO	PbS	13.1 ± 0.1	Null	3
	ZnO	PbS NC	12.44	Null	1
	Cs-ZnO	PbS	10.43	97%, after 3 months under 20 ° C and 30% RH without any encapsulation	1
	ZnO	CsPbBr ₃ -CsPb ₂ Br ₅	6.81	No detectable decay after 100 days under 25 °C and 45% RH	1
	ZnO	PTB7-Th:PC ₇₁ BM	12.02	Null	1
	Na-ZnO	p-DTS(FBTTh ₂) ₂ :PC ₇₀ BM	9.2	90%, after 28 h	1
	SnO_2	N719	3.2	Null	1
	Ni:SnO ₂		3.6		
	Zn:SnO ₂		4.2		
	SnO ₂	Eosin-Y	3.89	Null	1
	Sn _{0.92} O ₂ :Sb _{0.08}		4.15	Null	1

Table 2 (Contd.)

NC	Active layer	PCE (%)	Long-term stability	Ref
SnO_2	PBDR-T & ITIC-4	12.023	①>90%, up to 75 h after exposure to an ambient atmosphere with continuous illumination; ②>95%, after storage in N ₂ for 200 h with continuous illumination	157
	PM6:Y6	14.9	81%, after 15 days stored in the air at RM without encapsulation	158
	PTB7-Th:PC ₇₁ BM	10.30	Null	159
	PM7:ITC6-4F	13.93	Null	100
	PM7:11C0-4F PM6:Y6	15.38		
$Cl@SnO_2$	CsPbI ₃ NCs	14.5	94.3%, after 100 h light aging 80%, without encapsulation under 1-sun light soaking and 50% relative humidity for 8 h	27
Ga:SnO ₂	$Cs_{0.05}(MA_{0.17}FA_{0.83})_{0.95}Pb(I_{0.83}Br_{0.17})_3$	18.18	Null	161
SnO_2	CsPbI ₃ /FAPbI ₃	16.07	96%, after 1000 h in ambient storage	162
	$Cs_x(MA_{0.17}FA_{0.83})_{(100-x)}Pb(I_{0.83}Br_{0.17})_3$	17.92	89%, after 2500 h stored under 20 \pm 5% RH	163
	$MAPbI_3$	13.90 (flexible device)	Null	164
	$(CsPbI_3)_{0.04}(FAPbI_3)_{0.82}(MAPbBr_3)_{0.14}$	20.34 ± 0.5	90%, after 720 h storage	165
	$Cs_{0.05}(MA_{0.17}FA_{0.83})_{0.95}Pb(I_{0.83}Br_{0.17})_3$	20.79	Null	167
	$FAPbI_3$	25.39 (0.0803 cm ²)	①80% after 1000 h in ambient air at 25% RH and 25 °C without sealing; ②70.5% after 700 h light soaking; ③95% (encapsulated cell) after 100 h MPP tracking and 2 h dark recovery under ambient conditions	168
		23.3 (1	Null	
		cm ²)		
		21.7 (20 cm²)	Null	
		20.6 (64 cm²)	Null	
SnO ₂ /TiO ₂ (bilayer)	$\mathrm{CsPbI}_2\mathrm{Br}$	15.86	\bigcirc ~95%, after 1 month storage in N ₂ glovebox without encapsulation; \bigcirc >80%, after 1 month stored under RT and 20–30% RH without encapsulation	169
SnO ₂ /InP–ZnS (bilayer)	PM6:Y6	15.22	>80%, after 500 h in N ₂ without encapsulation	170
Ni:Co ₃ S ₄	N719	6.01	Null	171
Ni:Co ₄ S ₃		6.82		
$ m NiCo_2S_4$		7.43		
Zn_2SnO_4		4.9 ± 0.2		172
Y:SrSnO ₃	$FA_{0.85}MA_{0.15}Pb(I_{0.85}Br_{0.15})_3$	19.0	91%, after 1000 h stored in N_2	173

based NC-LHSCs, $^{30,32,35,39,40,44,45,58,131-145}$ PSCs, 146 and OSCs. $^{147-149}$ SnO NCs as ETL for DSSCs, $^{150-156}$ for OSCs, $^{157-159}$ and for PSCs, $^{27,160-168}$ have been demonstrated. Additionally, a bilayer of SnO₂/TiO₂ (ref. 169) and SnO₂/InP–ZnS¹⁷⁰ were used for PSCs and DSSCs. Ni-doped Co₃S₄ and Co₄S₃ and ternary sulphide NCs of NiCo₂S₄ and Zn₂SnO₄ have been used for DSSCs, 171,172 while

doped SrSnO₃ NCs for PSCs.¹⁷³ NCs have been used as IFL for NC-LHSCs,^{49,141,174-179} OSCs,¹⁸⁰⁻¹⁸⁵ DSSCs,¹⁸⁶⁻¹⁹⁵ PSCs,¹⁹⁶⁻²¹² and Si solar cells.²¹³⁻²²⁰ FAPbBr₃ perovskite NCs have been used as a multifunctional luminescent-downshifting passivation layer for GaAs solar cells.²²¹

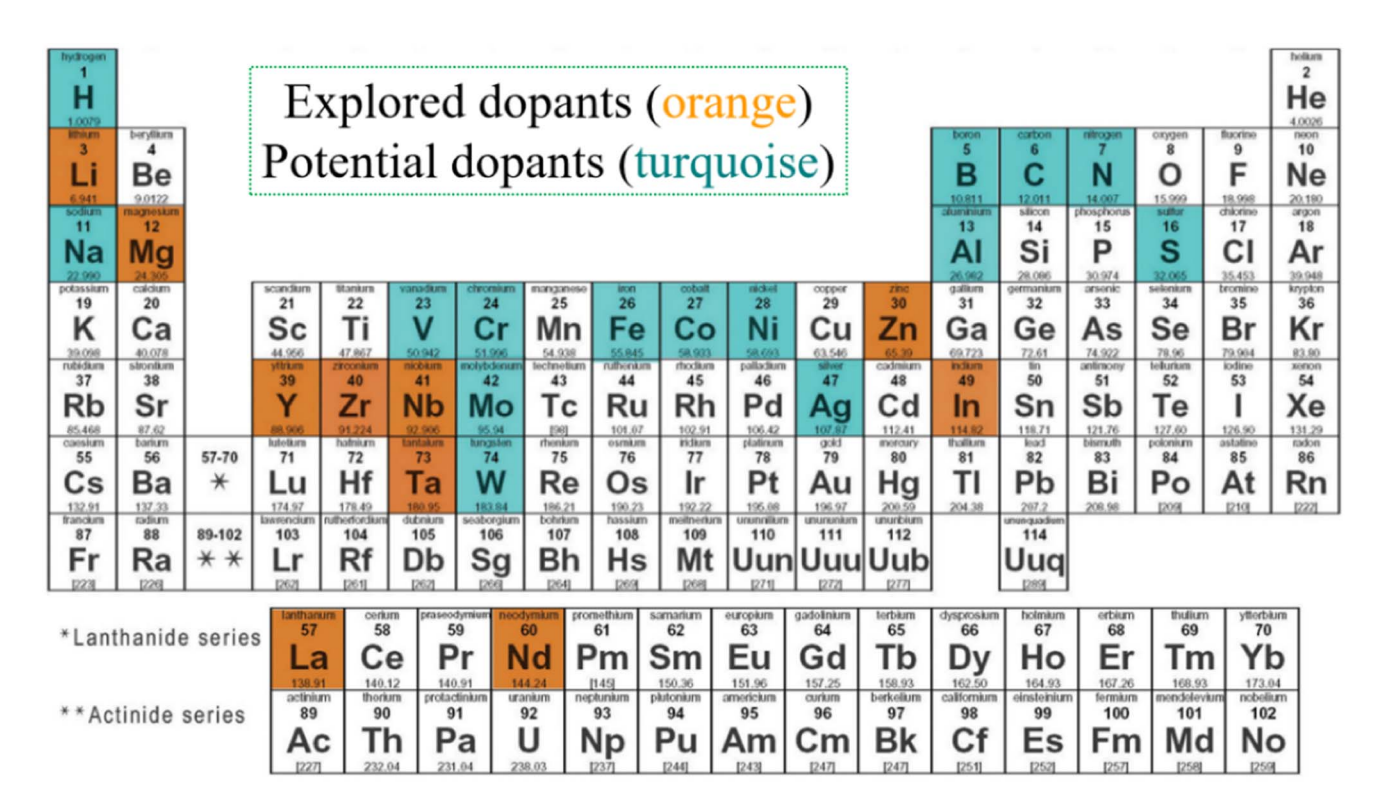


Fig. 6 Summary of the explored and potential elements as dopants in TiO_2 -based electron transporters for PSCs in the periodic table, as in 2017.²⁵³ Copyright 2017, Wiley-VCH.

From the reported literature listed in Table 2, selenide NCs of CdSe, and doped sulfide NCs of Ni: Co_2S_4 , Ni: Co_4S_3 , and Ni: Co_2S_4 have shown their potential, suggesting more substitutes for traditional NC ETL. The advantages of NC ETL and some potential NCs suitable as ETLs are discussed in the following sections.

2.2.2 Advantages of NC ETL. Compared with common organic ETLs such as fullerenes (C_{60}/C_{70}) and phenyl-C61-butyric acid methyl ester (PCBM), semiconductor NCs can easily overcome the shortcomings of poor stability, high cost, and unsuitable energy levels. In detail, PCBM film degrades at 85 °C, indicating its thermal instability. ¹¹⁰ The cost of synthesis and purification for organic electron transport materials is higher than most semiconductor NCs. ²⁵² Moreover, the semiconductor NCs can offer adjustable energy levels by easily

controlling the size. The above advantages strongly demonstrate that semiconductor NCs are a very good choice as efficient ETL in high-performance solar cells.

2.2.3 Potential NC ETL. Thanks to their unique application advantages in solar cells, NC ETLs have been widely used, boosting the devices to higher PCE and stability. More oxide and chalcogenide NCs as well as their doped congeners are anticipated alternatives. As we know, TiO₂NCs always act as splendid ETL in solar cells. The properties of TiO₂NCs can also be improved by doping, enhancing the device performance. As shown in Fig. 6, many elements were successfully doped in TiO₂ as ETL for PSCs. Meanwhile, more elements are potential dopants for high-quality TiO₂ and this suggests that there is much room for doped-TiO₂NC ETL. Additionally, we reasonably

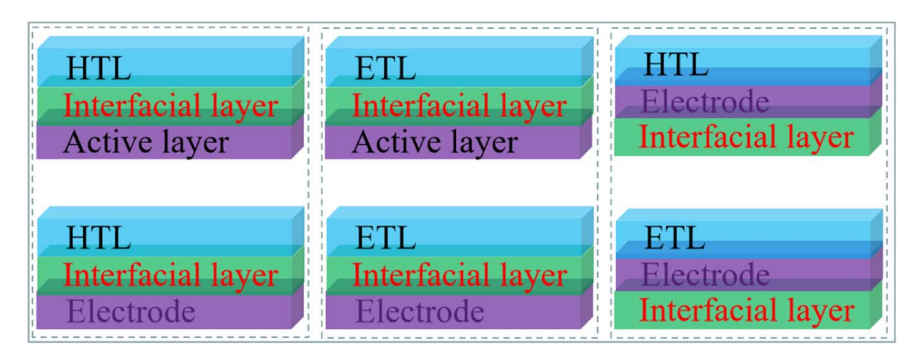


Fig. 7 Typical position sketch of interfacial layers in solar cells.

Table 3 Recent advances in selected NCIFLs

	IFL and its adjacent layers	PCE (%)	Functions	Ref.
PbCdS	TiO ₂ /PbCdS/CdS	3.35	Enhance light absorption; suppress interfacial recombination	174
CdS + amine/ZnS	TiO ₂ :Al ³⁺ /CdS + amine/ZnS/ electrolyte/CuS	2.4	Decrease electron-hole recombination	175
Cu_xS	CIZS + mp-TiO ₂ /electrolyte/Cu _x S/ electrode	1.13	Null	176
CdSe	ZnO/CdSe/PbS	7.9	Suppress interface recombination; contribute additional photogenerated carriers	141
NiO	PbS-EDT/NiO/Au	10.4	Improve hole extraction efficiency; suppress the penetration of moisture and oxygen; good band alignmen	49 t
PbS-EDT	PbS-TBAI/PbS-EDT/P3HT	8.7	Adjust the valence band; improve charge transfer	177
CsPbBr ₃	PbSe-MPA/CsPbBr ₃ /Au	7.22	Suppress carrier recombination	178
ZnO	Mg-doped ZnO/ZnO/PbS	7.06	Decrease the interface recombination	179
CdSe	ZnO/CdSe/P3HT:PCBM	2.25	Increase conductivity; electron transport and hole block	180
CuInS ₂ -ZnS	TiO ₂ /CuInS ₂ -ZnS/PCDTBT:PC ₇₁ BM	7.01	Increase the electron extraction; reduce impedance	181
CdSe	P3HT:PCBM/CdSe/Al	3.08	Down-conversion, reduce charge recombination	182
ZnCdS	TiO ₂ /ZnCdS/PTB7:PC ₇₁ BM	7.75	Suppress the recombination; reduce the series resistance	183
SnO ₂	ITO/SnO ₂ /ZnO	7.16	Enhance optical transmission; reduce energy barrier; suppress carrier recombination	184
Ag ₂ Se	TiO ₂ /Ag ₂ Se/N719	5.89	Null	186
CdS	TiO ₂ /CdS/N719	7.54	Suppress the charge recombination; increase the optical absorption	187
CeO ₂ :Eu ³⁺	N719/CeO ₂ :Eu ³⁺ /electrolyte	8.36	Down-convert UV light to visible light, light scattering	190
NaGdF ₄ :Eu ³⁺	FTO/TiO ₂ /N719/electrolyte/Pt/FTO/ NaGdF ₄ :Eu ³⁺	9.34	Act as luminescent down-conversion centers and light scatterers in the ultraviolet and visible domains	191
CaCe ₂ (MoO ₄) ₄ :Er ³⁺ /Yb ³⁺	Electrolyte/CaCe ₂ (MoO ₄) ₄ :Er ³⁺ /Yb ³⁺ / Pt	7.78	Convert the NIR and UV radiation to visible emissions	192
NaYF ₄ :20%Yb, 2% Er@NaYF ₄ :7%Eu	N719/NaYF ₄ :20%Yb,2% Er@NaYF ₄ :7%Eu/Pt	7.664	Convert NIR and UV lights to visible lights	193
SrF ₂ :Pr ³⁺ -Yb ³⁺	FTO/SrF ₂ :Pr ³⁺ -Yb ³⁺ /TiO ₂ -N719	9.07	Absorb blue light and emit green and red light	194
BaWO4:Pr ³⁺	TiO ₂ /BaWO4:Pr ³⁺ /N719	8.08	Absorb UV light and emit blue, green, and red light	195
MAPbBr _{0.9} I _{2.1}	$TiO_2/MAPbI_3/MAPbBr_{0.9}I_{2.1}$	13.32	Facilitate hole transfer from MAPbI ₃ to HTL	196
CuInS	MAPbI ₃ /CuInS/spiro-MeOTAD	13.8	Enhance charge transfer; suppress charge recombination pathways	
MgO	${\rm FTO/MgO/SnO_2}$	18.23	Smoother surface; less FTO surface defects; suppressed electron–hole recombination	199
CdS	TiO ₂ /CdS/MAPbI ₃	10.52	Longer electron lifetime; lower charge carrier recombination rate	200
SnO_2	PC ₆₁ BM/SnO ₂ /Al	19.7	Block holes; enhance the conductivity; reduce the recombination	201
Cl-SnO ₂	FTO/Cl-SnO ₂ /CsMAFAPbI ₃ Br _{3-x}	17.3	Fill the pinholes; passivate the trapping defects	202
FAPbX ₃	MAPbI ₃ /FAPbX ₃ /C60	7.59	Enhance absorption	203
PbS	MAPbI ₃ /PbS/spiro-OMeTAD	19.24	Enhance hole extraction; retard interfacial recombination improve perovskite film morphology	
CuO_x	NiO _x /CuO _x /MAPbI ₃	19.91	Lead higher transfer efficiency and lower carrier recombination	205
$MAPbBr_{0.9}I_{2.1}$	SnO ₂ /MAPbBr ₃ /MAPbBr _{0.9} I _{2.1}	20.21	Optimize the energy level; improve hole extraction	206
Co-CuGaO ₂	Cs _{0.05} (MA _{0.15} FA _{0.85}) _{0.95} Pb(I _{0.85} Br _{0.1} 5) ₃ / Co-CuGaO ₂ /spiro-OMeTAD		Reduce the energy gap; prevent direct contact between PVK and oxygen and moisture	
MoS ₂ :RGO	MAPbI ₃ /MoS ₂ :RGO/spiro-OMeTAD	20.12	Extract holes and block electrons	208
CsCu ₅ S ₃	MAFAPbI ₃ /CsCu ₅ S ₃ /spiro-OMeTAD	22.29	Favor for energy levels; reduce carrier recombination	209
Cu _{2-x} S@SiO ₂ @Er ₂ O ₃	TiO ₂ /Cu _{2-x} S@SiO ₂ @Er ₂ O ₃ /MAPbI ₃	17.8	Upconvert infrared light to visible light	210
$NaYF_4:Yb^{3+},Er^{3+}/$	IR-783 + NaYF ₄ :Yb ³⁺ ,Er ³⁺ /	20.5	Convert IR to visible light, scatter light	212
$\text{@NaYF}_4:\text{Yb}^{3+},\text{Nd}^{3+}$	@NaYF ₄ :Yb ³⁺ ,Nd ³⁺ + Au/ CsMAFAPbBrI	20.0	Somete In to visible again seatter again	-12
MoS_2	$SiO_x/MoS_2/MoO_x$	22.8	Provide electron-blocking and hole-extraction properties	213
PbS	PbS/c-Si solar cell	12.6	Luminescent solar concentrator	214
CdS	Si solar cell/CdS	9.37	Reduce the reflectance spectral ranging from 250 to	216
		- 101	1100 nm, passivation, and down-conversion	_10

Table 3 (Contd.)

	IFL and its adjacent layers	PCE (%)	Functions	Ref.
$Zn_xCd_{1-x}S-ZnS:Mn$	Si solar cell/Zn _x Cd _{1-x} S-ZnS:Mn	14.271 ± 0.268	Down-conversion	217
Cd _{0.5} Zn _{0.5} S–ZnS:Mn	Si solar cell/Cd _{0.5} Zn _{0.5} S–ZnS:Mn	17.90	Down-convert UV light of 250–450 nm to yellow-orange light at 583 nm	218
NaGdF ₄ :Ce@NaGdF ₄ :Nd/	c-Si solar cell/	0.8 (under	Expand the spectrum of quantum cutting in the NIR	219
Yb@NaYF ₄	$NaGdF_4{:}Ce@NaGdF_4{:}Nd/Yb@NaYF_4\\$			
$CsPbCl_{1.5}Br_{1.5}$: Yb^{3+} , Ce^{3+}	c-Si solar cell/CsPbCl _{1.5} Br _{1.5} :Yb ³⁺ ,Ce ³⁺	illumination) † 21.5	Larger absorption cross-section, weaker electron-phonon coupling and higher inner luminescent quantum yield	220

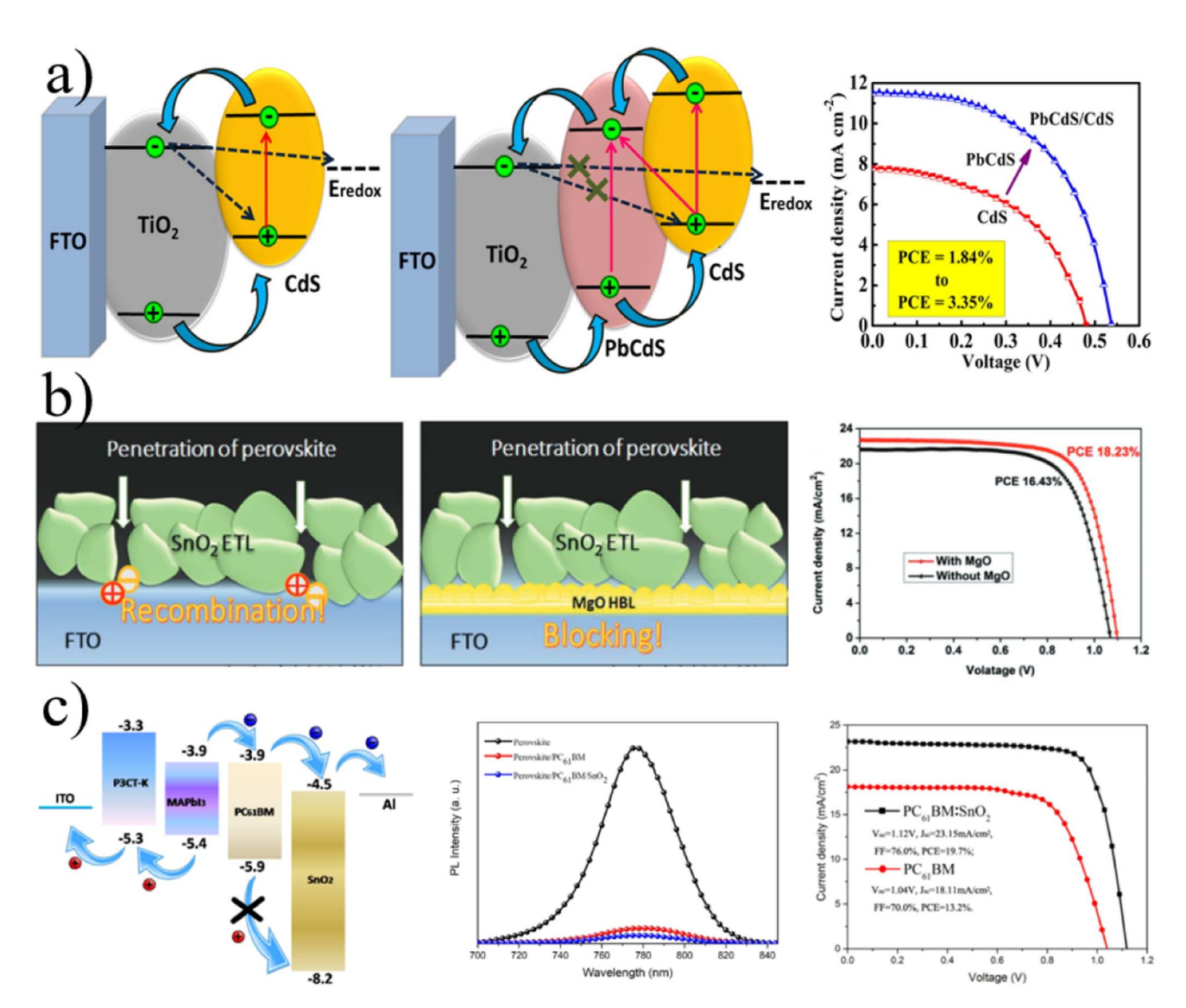


Fig. 8 (a) Schematic illustration of the possible electron transfer process in bare CdS and PbCdS/CdS based solar cells and J-V curves of CdS and PbCdS/CdS based solar cells. (b) The perovskite can directly contact the FTO surface along a shunt pathway in the absence of SnO₂ ETLs; the MgO₂ layer can inhibit the penetration of perovskite reaching the FTO surface, and the best performance of the PSCs with and without MgO. (c) Corresponding energy level diagram of PSCs, steady-state PL spectra of the perovskite film deposited on the PC₆₁BM layer and PC₆₁BM:SnO₂ bilayer, J-V characteristics in the illumination for the devices based on the PC₆₁BM layer and PC₆₁BM:SnO₂ bilayer. (a) Adapted with permission.¹⁷⁴ Copyright 2017, Elsevier. (b) Adapted with permission.¹⁹⁹ Copyright 2017, Wiley-VCH. (c) Adapted with permission.²⁰¹ Copyright 2018, American Chemical Society.

Nanoscale Advances Review

think this strategy is also applicable to other oxide NCs like SnO₂ due to its comparable nature with TiO₂.

3. Nanocrystals as IFL

Besides HTL and ETL, another essential layer is the interfacial functional layer (IFL). Interfaces play a non-ignorable role in improving both PCE and stability through many paths. The position of a typical IFL is shown in Fig. 7. The IFL can be located at different positions in the solar cells to make different contributions. NCs IFL can enhance light absorption, decrease carrier recombination, improve charge transport ability, reduce impedance, convert ultraviolet (UV) or near-infrared (NIR) light to visible light, enhance optical transmission, decrease trap states of the active layer, and so on. Table 3 shows the recent advances of NC IFLs, and the detailed discussion is as follows.

3.1 Suppressing recombination

As shown in Fig. 7, IFL is a separate layer between the charge transport layer/active layer or charge transport layer/electrode. So, it can convincingly act as a functional layer to prevent hole-electron recombination. Ternary semiconductor NCs of PbCdS were deposited on TiO2 as an IFL to impede the direct contact between ETL and the active layer of CdS, thus suppressing recombination efficiently and boosting the device PCE significantly (Fig. 8a). As the same, oxide NCs of MgO and SnO₂

film inserted between ETLs and electrodes blocked holes and reduced recombination (Fig. 8b and c). 199,201

3.2 Charge transport improvement

As we know, charge transport ability inevitably affects the performance of solar cells. As shown in Fig. 9a, MAPbBr_{0.9}I_{2.1}-NCs with good energy alignment enhance the hole transport ability and the PCE of the PSCs. Co-CuGaO₂ NCs with ~20 nm size were synthesized by hydrothermal method and used for surface passivation at the interface of perovskite and spiro-OMeTAD. Furthermore, the larger bandgap and lower valence band energy of Co-CuGaO2 reduced the energy gap between Co-CuGaO₂ and perovskite. Considering that the reduced energy gap improved hole conduction and electron blocking, the PCE of PSCs was enhanced from 18.60% to 20.39%. 207 MoS2NCs were also used to improve hole transport and the device PCE and stability (Fig. 9b).

Light conversion and harvest enhancement

It is known that the active layer of recent solar cells cannot respond to the whole solar spectrum, resulting in energy loss and relatively low efficiency. Broadening the absorption of the active layer is an efficacious strategy to reduce energy loss and enhance the performance of solar cells. CdS NCs with general Stocks shifts were used in Si solar cells for spectral range

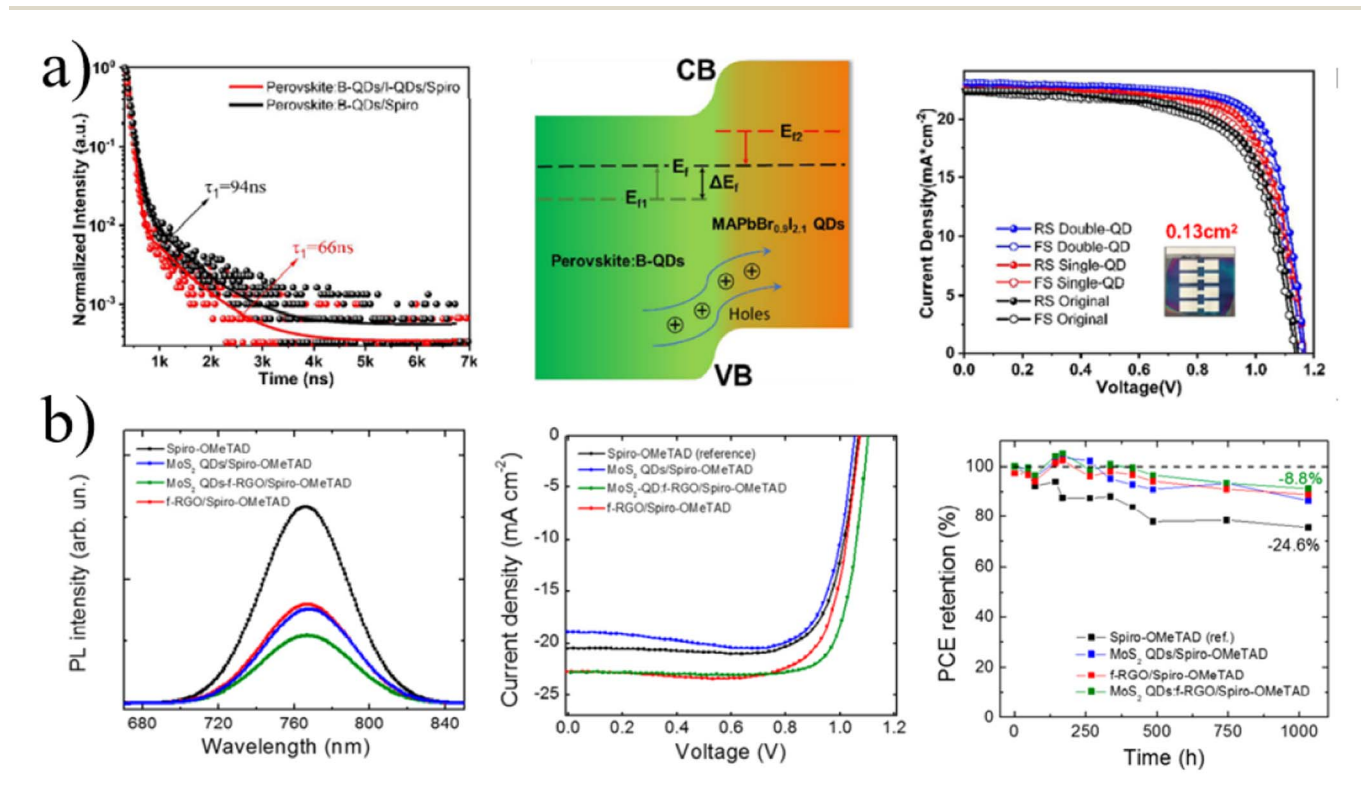


Fig. 9 (a) TRPL spectra of the perovskite film with and without MAPbBrl₂ NCs, schematic diagram of band bending in the heterojunction structure formed by the perovskite and MAPbBrl₂ NCs. (b) Steady-state PL measurements of MAPbl₃ after the deposition of spiro-OMeTAD and different IFL/spiro-OMeTAD, I-V characteristics of tested PSCs using different IFLs, normalized PCE trends vs. time extracted by I-V characteristics under 1 sun illumination, periodically acquired during the shelf life test for the PSCs. (a) Adapted with permission.²⁰⁶ Copyright 2020, American Chemical Society. (b) Adapted with permission.²⁰⁸ Copyright 2018, American Chemical Society.

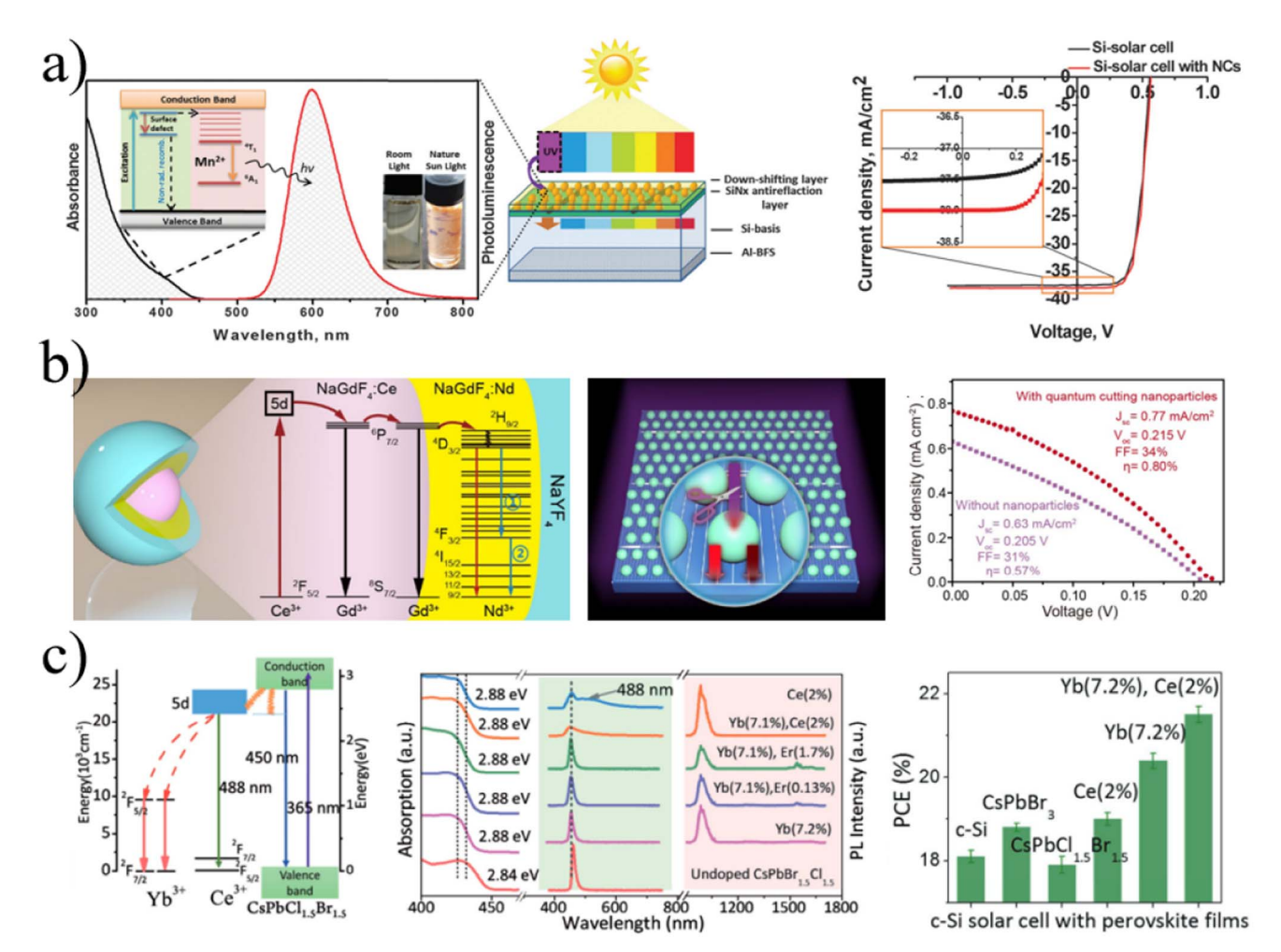


Fig. 10 (a) Scheme of the down-shifting mechanism of the $Zn_{0.5}Cd_{0.5}S$:Mn (5%)/ZnS NC converter material and the design of proof-of-concept solar cell; J-V curves of the corresponding solar cells. (b) Schematic and proposed energy transfer for Ce^{3+} -sensitized quantum cutting in Nd^{3+} ions; schematic design for boosting the energy-harvesting efficiency of c-Si solar cells with quantum cutting nanocrystals; comparison of current density-voltage characteristic for c-Si solar cells with and without a nanocrystal coating layer (the solar cells were illuminated with a 254 nm UV lamp at a power density of 7 mW cm⁻²). (c) Schematic diagram of energy transfer mechanism in the Yb^{3+} , Ce^{3+} codoped $CsPbCl_{1.5}Br_{1.5}NCs$, absorption; visible and near-infrared emission spectra of $CsPbCl_{1.5}Br_{1.5}$ perovskite NCs codoping with different rare earth ions; PCE of Si solar cells with different perovskite NCs. (a) Adapted with permission.²¹⁷ Copyright 2016, the Royal Society of Chemistry. (b) Adapted with permission.²¹⁸ Copyright 2017, Wiley-VCH.

enhancement.²¹⁶ In Fig. 10a, we can see that Mn-doped NCs expand the spectral range response of solar cells by absorbing short-wave lights and emitting the characteristic light around 580 nm, suggesting a larger range of light harvesting by active layer and PCE improvement. Zn_xCd_{1-x}S/ZnS:Mn²⁺ NCs were also used to broaden the light response range of Si solar cells.²¹⁷ Furthermore, Mn-doped semiconductor NCs have a large Stocks shift, avoiding self-absorption and thus reducing energy loss. Sr₂CeO₄ NCs with down-shifting properties could improve the stability of organic P3HT:PCBM solar cells without significant loss of short-circuit current.¹⁸⁵ Certainly, by using NCs with a Stocks shift for expanded light harvesting, the photoluminescence yield and other photoelectronic properties should keep the rules of high-performance solar cells.

Besides the above NCs, rare elements are good at light conversion due to their special energy levels. Undoped and doped NCs based on rare elements were massively applied to broaden the light response in solar cells and efficiently boost the device performance. As seen in Fig. 10b and c, Yb³⁺, Ce³⁺, and Nd³⁺ based NC layers efficiently convert light and enhance the device performance. Additionally, Eu³⁺, Er³⁺, and Pr³⁺ were also used for efficient solar cells.

3.4 Energy level optimization

To ensure propitious charge transfer among the functional layers in solar cells, un-matched energy levels are a tricky issue that we need to address. One origin of the open-circuit voltage (V_{oc}) loss of NC-LHSC, Si solar cells, PSCs, and OSCs is mainly analyzed quantitatively via the energy difference between bandgap and the Schokley–Queisser limit voltage. For n-i-p solar cells, band alignment between the active layer and ETL directly limits the splitting of the quasi-Fermi level. For p-i-n solar cells, the band alignment between HTL and active layer has a great impact on the V_{oc} . The conduct band of recent HTL

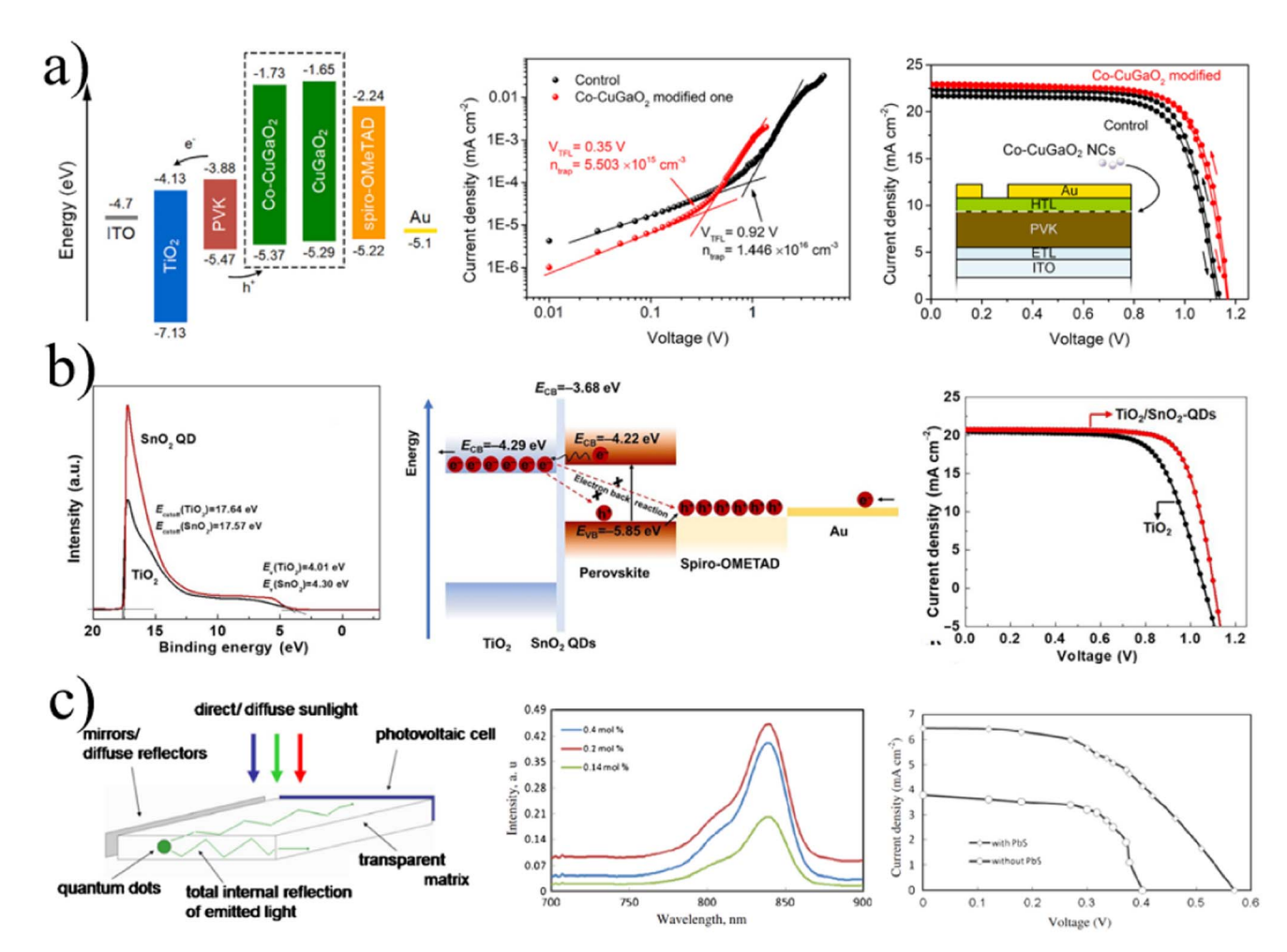


Fig. 11 (a) Energy level diagram of PSCs with the ITO/TiO2/PVK/Co-CuGaO₂/spiro-OMeTAD/Au structure, dark I-V curves of devices based on spiro-OMeTAD and Co-CuGaO₂/spiro-OMeTAD, forward and reverse scan J-V curves based on spiro-OMeTAD and Co-CuGaO₂/spiro-OMeTAD. (b) Band edge alignment and photocarrier dynamics in the resultant device. (c) Schematic illustration of an NC-luminescent solar concentrator, PL spectra of PbS NC-luminescent solar concentrator with different concentrations of PbS, and J-V curves for solar cells with and without PbS NC-luminescent solar concentrator. (a) Adapted with permission.²⁰⁷ Copyright 2022, Elsevier. (b) Adapted with permission.²⁰⁸ Copyright 2019, Elsevier. (c) Adapted with permission.²¹⁵ Copyright 2015, Springer.

is relatively deep, and the barrier for electron transport is not sufficient, resulting in electron leakage and reducing the device performance. Therefore, energy level is of great importance to improve the performance of solar cells. Shown in Fig. 11a and b, Co-doped CuGaO $_2$ and SnO $_2$ NCs film were used for energy level optimization for high-performance solar cells, illuminating the large potential of NCs as ITL for reducing $V_{\rm oc}$ loss of solar cells.

3.5 Concentrating luminescent solar radiation

Solar radiation is geographically extensive, but the energy density is not high. So, concentrating solar light for higher density is a feasible strategy to improve solar cell performance. PbS NC luminescent solar concentrator (LSC) was found to show potential advantages over silicon solar cell panels (Fig. 11c). They can reduce the size of solar cells and offer great flexibility in design, which results in cost reduction with any desired shape. One of the attractive LSCs is based on NCS.

3.6 Prevention

The main reason for unstable solar cells is the invasion of oxygen and water. IFL between the active layer and HTL, ETL, or electrode can arrest this invasion to a great degree and increase the stability of solar cells. The above-mentioned IFL of Co-CuGaO₂ NCs in Fig. 11a not only acts as a hole transport accelerator but also prevents the direct contact of perovskite with oxygen and moisture, boosting the stability of the PSCs.²⁰⁷

4. Nanocrystals as efficient additives

Besides an independent layer to improve the performance of solar cells, NCs have also been used as additives for boosting active layer quality, carrier transfer acceleration, spectral response broadening due to plasmonic effect, light conversion, light scattering/reflection, heat sinking, and some other functions. Table 4 lists the recent progress of NCs as efficient additives for high-performance solar cells.

Table 4 Recent advances in NC additives for high-performance solar cells

NC	Added layer	NC additives and the mixture	PCE (%)	Functions	Ref.
SnO ₂ –Sb ₂ O ₃	Bottom ETL	SnO_2 - Sb_2O_3 + TiO_2	7.7	①Improve the electron mobility and light harvesting; ②avoid the recombination	222
PbS		PbS + m-TiO ₂	5.04	①Enlarge the grain size of CsPbBr ₃ perovskite film; ②suppress the activation of intrinsic trap sites of m-TiO ₂	223
		${\rm PbS} + {\rm TiO}_2$	14.95	Downshift the conduction band of TiO ₂ , promote the driving force of an electron injection	227
Cu-Zn-In-S-Se (CZISSe)		$CZISSe + mp-TiO_2 + CsPbBr_3$	5.37	①Enhance charge extraction; ②reduce charge recombination	225
Ho ³⁺ –Yb ³⁺ –F [–] tri-doped TiO ₂		$\mathrm{Ho^{3^+}\!\!-\!Yb^{3^+}\!\!-\!F^-}$ tri-doped $\mathrm{TiO_2}$ + $\mathrm{TiO_2}$	9.91 ± 0.3	Convert NIR light to green light	232
$Gd_{1.54}Er_{0.46}(MoO_4)_3$ (GMO:Er)		GMO:Er + TiO ₂	3.41	Convert NIR light to the visible region (near 550 nm)	233
β-NaYF ₄ :Yb ³⁺ /Er ³⁺ / Sc ³⁺ @NaYF ₄		β-NaYF ₄ :Yb ³⁺ /Er ³⁺ /Sc ³⁺ @NaYF ₄ + TiO ₂	20.19	Convert NIR to red and green light	243
SrAl ₂ O ₄ :Eu ³⁺		$SrAl_2O_4$: $Eu^{3+} + TiO_2$	4.64	Elevation of the Fermi energy level of TiO ₂ , improves light harvesting	245
ZnSTe	Bottom HTL	ZnSTe + PEDOT:PSS	2.31	Reduce series resistance, increase shunt resistance, improve mobility	230
NaCsWO ₃ @NaYF ₄ @ NaYF ₄ :Yb,Er	Top HTL	NaCsWO ₃ @NaYF ₄ @NaYF ₄ :Yb,Er + spiro	18.28 ± 0.34	①Widen the perovskite spectral response range; ②increase the light reflection; ③ prolong the light path, and light absorption	231
NaLuF ₄ :Yb,Er@NaLuF ₄		${\tt NaLuF_4:Yb,Er@NaLuF_4+PTAA}$	15.86	Convert NIR light to visible light, scatter light	237
Li(Gd,Y)F ₄ :Yb,Er		$Li(Gd,Y)F_4:Yb,Er + spiro-MeOTAD$	18.34	Convert NIR to visible light	242
SnO_2	Active layer	$SnO_2 + P3HT-PCBM$	3.39	Reduce the recombination	224
Fe-doped SnO ₂		Fe-doped SnO_2 + P3HT	3.04	Extension of photogenerated exciton lifetime, overcome the burn-in regime faster	247
NaYF ₄ :Yb,Er/NaYF ₄		NaYF ₄ :Yb,Er/NaYF ₄ + N719	9.15	Convert NIR light to visible light (450–700 nm)	235
TiO ₂ :Sm ³⁺		$TiO_2:Sm^{3+} + P25 + N719$	5.31	Convert UV to visible light	244
SnS		${\rm SnS} + {\rm MAPbI}_3$	14.26	①Provide more nucleation sites for the growth of perovskite grains; ② accelerate carrier transfer and reduce the recombination	226
NaYF ₄ :Yb/Er		${\bf NaYF_4:} {\bf Yb,} {\bf Er} + {\bf MAPbI}_3$	17.8	Broaden the solar spectral use to NIR light, minimize the non- absorption energy loss	236
IR-806-β-NaYF ₄ :Yb,Er		IR-806-β-NaYF ₄ :Yb,Er + MAPbI ₃ Er ³⁺ -Yb ³⁺ doped Zn	17.49	Convert NIR light (800–1000 nm) to visible emissions	238
Ho ³⁺ –Yb ³⁺ –Li ⁺ -doped TiO ₂		${ m Ho^{3^+}-Yb^{3^+}-Li^+}$ -doped ${ m TiO_2}$ + FAMAPbBrI $_3$	16.88 ± 0.5	Convert NIR to visible light, improve electron injection efficiency, and decrease recombination	240
β-NaYF ₄ :Yb ³⁺ ,Tm ³⁺ @TiO ₂		$β$ -NaYF $_4$:Yb $^{3+}$,Tm $^{3+}$ @TiO $_2$ + MAPbI $_3$	16.27	Convert NIR to visible light, serve as the light scatter centers	241

4.1 Active layer quality improvement and carrier transfer accelerator

The performance of solar cells largely depends on the quality of the active layer, such as the purity of Si for Si solar cells and the composition of perovskite for PSCs. For example, defects unavoidably exist at the surface of perovskite thin film during

the low-temperature fabrication process, and reducing defects is a very useful way to improve the performance of PSC.²⁵⁴ This subsection discusses NCs as outstanding additives in the active layer for boosting its quality and carrier transfer acceleration.

SnO₂-Sb₂O₃ NCs were used to modify TiO₂ nanorod arrays for electron mobility improvement and electron transport

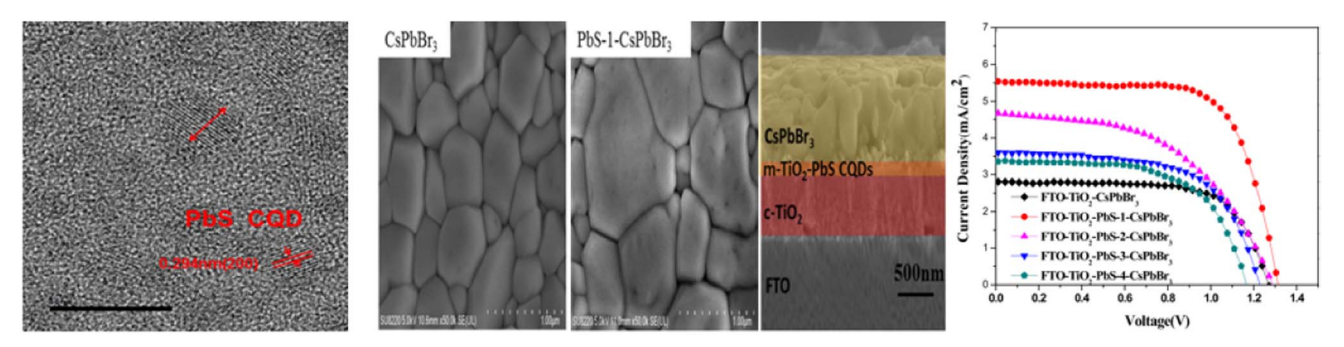


Fig. 12 Top-view and cross-section images of CsPbBr₃ film decorated with PbS NCs, and J-V curves of all-inorganic PSCs based on different TiO/PbS photoanodes. Adapted with permission.²⁴³ Copyright 2019, American Chemical Society.

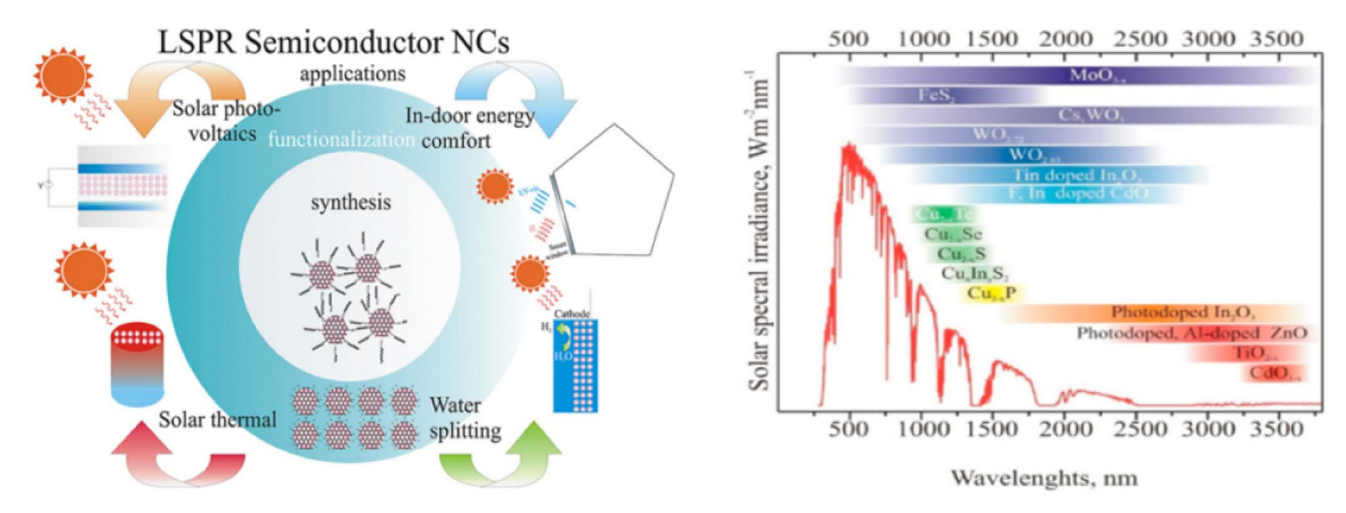


Fig. 13 Schematic of the applications of LSPR semiconductor NCs; the solar spectrum and its relevancy for energy-targeted applications of LSPR semiconductor NCs via their tunable plasmon absorbance. Adapted with permission.²⁵⁵ Copyright 2021, Elsevier.

resistance reduction. This NCs modified ETL enhanced the PCE of CH₃NH₃PbI_{3-x}Cl_x PSC from 6.5% to 7.7%.²²² PbS NCs suppress the activation of the intrinsic trap sites, provide nucleation sites to enlarge the grain size, and suppress the charge combination in CsPbBr₃ PSCs (Fig. 12).²²³ Adding SnO₂ NCs of size around 5 nm into the active layer of P3HT:PC61BM made electrons more easily pass through the active layer and accelerate the electron transfer, improving the PCE of OSC from 2.67% to 3.39%.224 S2O32-capped Cu-Zn-In-S-Se NCs with \sim 5 nm size was introduced in the perovskite precursor of PbBr₂ solution to boost 22.6% enhancement of the PCE of inorganic Cs-based PSCs, which was due to promoted crystallization of CsPbBr₃ and hole extraction.²²⁵ SnS NCs with an average size of 6.9 nm were implanted into the active layer of carbon-based HTL-free mesoporous PSCs, and the device gained a high PCE of 14.26% with a 12.42% improvement. This improvement was demonstrated by more nucleation sites for the growth of perovskite grains and the accelerated carrier transfer.²²⁶ PbS NCs doped TiO₂ nanotubes (TNTs) modified the electronic and optical properties by downshifting the conduction band of TiO₂ ETL from -4.22 to -4.58 eV and promoting the driving force of an electron injection to the conductive electrode.227

4.2 Plasmonic Effect

Semiconductor NCs have exhibited localized surface plasmon resonances (LSPR), and this plasmonic effect has been used in many fields, such as solar photovoltaics, in-door energy comfort, water splitting, and so on (Fig. 13). Compared with traditional LSPR materials (noble metals), the semiconductor LSPR NCs allow a wide range of wavelength tunability from visible towards near-infrared (NIR) and further to mid-IR, leading to larger absorption of solar light. Higher absorption of the active layer in solar cells increases the current intensity and thus, the device performance. DSSCs based on plasmonic effect by ZnO or SnO2 and TiO2/SnO2 have been investigated.254 From Fig. 13, it can be seen that different oxides, sulfides, and selenides such as MoO_{3-x} , Cs_xWO_3 , TiO_{2-x} , CdO_{1-x} , doped In_2O_3 , doped ZnO, $Cu_{2-x}S$, $Cu_xIn_yS_2$, $Cu_{2-x}Se$, etc. broaden the response spectra from 500 nm to nearly 3800 nm. Effective light harvesting due to the plasmonic effect shows great potential in solar cell application. Given the limited self-absorption bands of solar cells, the above oxide and sulfide NCs can be applied as additives to widen the light harvesting range. Clearly, this will reduce energy loss and raise the device performance in a considerable way.

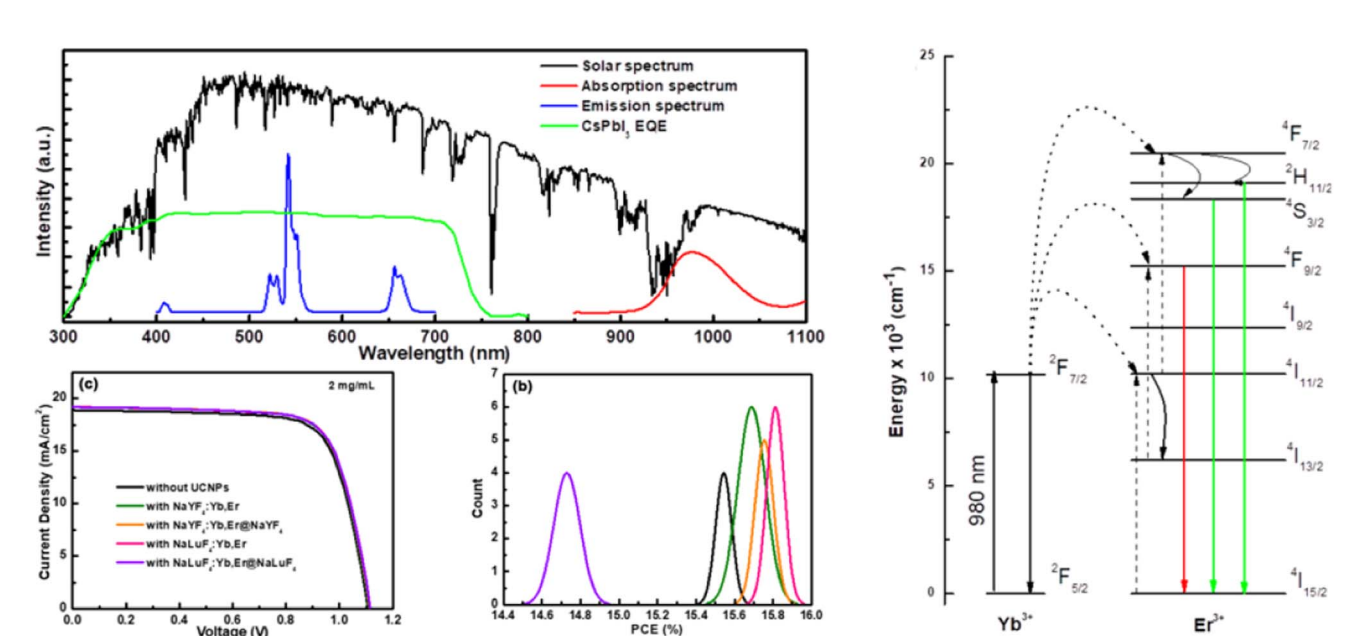


Fig. 14 Solar spectrum, absorption and emission spectrum of up-conversion nanocrystals and EQE curve of γ -CsPbl₃ PSC, J-V curves of PSCs based on different nanocrystals, and statistical PCE distribution histograms of 30 devices, schematic energy diagram for Yb³⁺ and Er³⁺. Adapted with permission.²³⁷ Copyright 2019, American Chemical Society.

4.3 Light conversion

Review

As discussed in Section 3, light conversion is an efficient way to boost the PCE and stability of solar cells. Based on this point, NC light-converting layers were investigated in the previous part. It is also true that light conversion can be realized by NC additives, which will be summarized in this part.

4.3.1 Up-conversion. Rare-earth (RE) elements are famous for light up-conversion and further application in solar cells. RE element-doped semiconductor NCs have been added as additives in active layers and charge transport layers for highperformance DSSCs and PSCs. NIR lights were up-converted to visible lights and thus elevated the device PCE due to wider solar radiation absorption (Fig. 14). The RE element-based NCs, which can be used in up-converting materials as additives in solar cells, mainly contain Yb, Er, Ho, and Sc doped materials like Ho-Yb-F doped TiO2, Er-Yb doped ZnO2, Ho-Yb doped Gd₂O₃, Yb-Er doped NaYF₄ and Yb-Er doped Li(Gd,Y)F₄. As shown in Fig. 14, the schematic energy diagram for Yb³⁺ and Er³⁺ are suitable for up-conversion and the related solar cells gain high efficiency. The up-conversion NCs can be added in the active layer, ETL, and HTL in different solar cells like OSC, DSSC, and PSC. The original active layers cannot absorb the whole range of sunlight and thus result in energy loss. After assembling NCs with up-conversion ability, the non-responsive long-wavelength range of sunlight will be converted to shorter wavelengths and absorbed by active layers to re-generate holeelectron pairs. This strategy can enhance the utilization of the infrared range of sunlight and the performance of solar cells.

4.3.2 Down-conversion and down-shifting. Down-conversion and down-shifting NCs are advantageous for high-performance solar cells due to the efficient utilization of UV lights. Typical Sm³⁺-based TiO₂NCs were used in DSSCs and obvious improvement of PCE was gained (Fig. 15) through

converting ultraviolet to visible light. Better performance of solar cells was obtained by means of down-converting NCs such as ZnS:Er in Si-based devices and CeO₂:Gd in OSC. ^{249,250} The shortest wavelength response by perovskite is about 400 nm. ²⁵⁶ The energy of sunlight with wavelengths shorter than 400 nm will be wasted. Furthermore, the UV lights can damage the perovskite or organic active layer and reduce the device stability. So, the PCE and light stability of solar cells can be increased by using down-conversion or down-shifting NCs.

4.4 Light scattering and reflection

Light scattering and reflection are well-known for boosting the optical absorption of different solar cells. TiO₂:Zn NCs can scatter light and promote the performance of conventional DSSCs.²⁵⁷ Due to the ultralow (<1%) photoluminescence quantum yield, NaLuF₄:Yb,Er@NaLuF₄NCs acted as scattering centers and extended the sunlight optical path by combining scattering and reflecting sunlight.²³⁷ NaYF4:Yb³⁺,Tm³⁺ NCs serve as scatter centers to enhance light harvesting for PSCs.²⁴¹ We can conclude that NCs are good at light absorption enhancement due to light scattering and reflecting, and this is an available approach for improving the device performance.

4.5 Heat sinks

Except for optical management, heat control is also important for solar cell operation because elevated temperatures may increase energy loss and destroy the devices. In the traditional photovoltaic/thermal (PV/T) system, the temperature of thermal energy is always limited by the operation temperature of PV cells. The oleylamine solution of $\text{Cu}_9\text{S}_5\text{NCs}$ was adopted in the spectral splitting filter to harvest the moderate-temperature heat. After successful thermal energy collection, the maximum

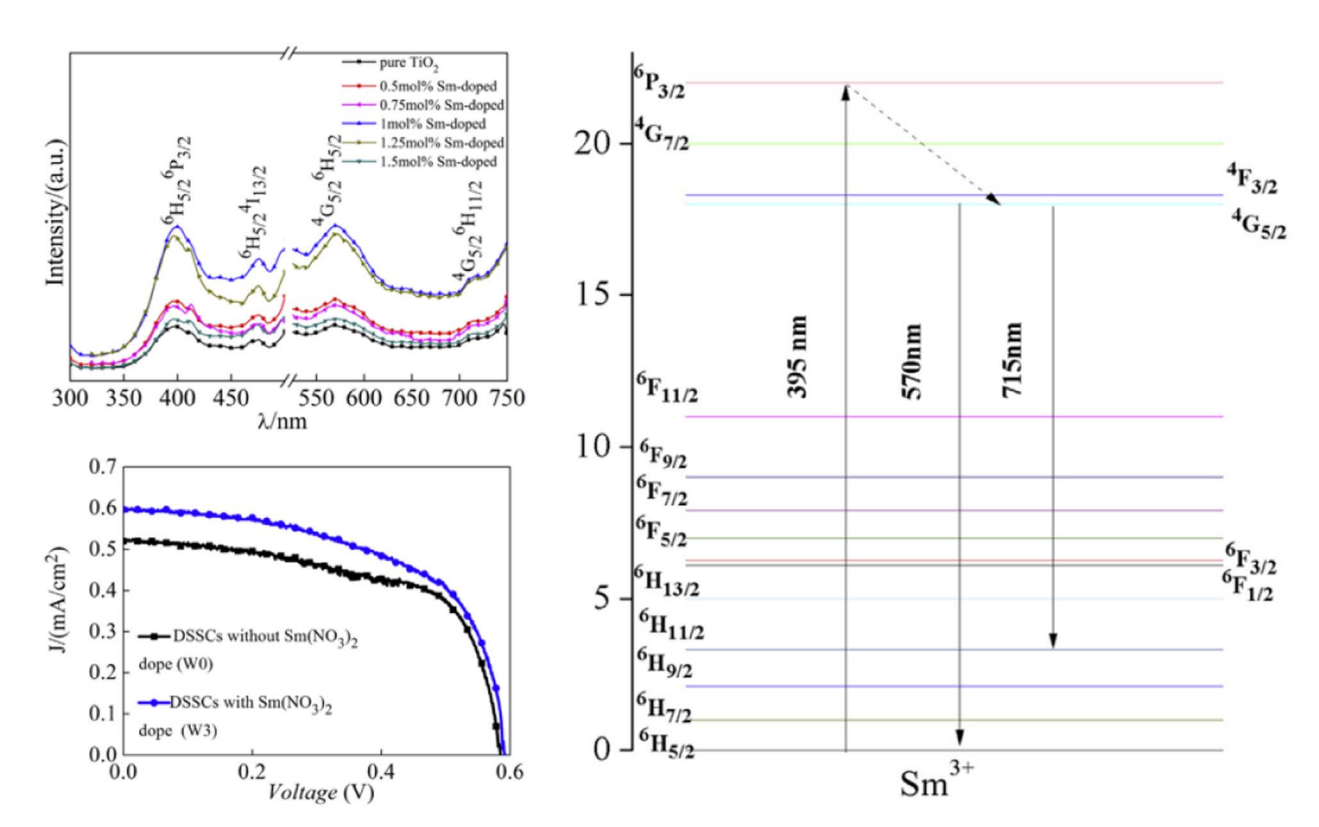


Fig. 15 Excitation spectrum ($\lambda_{em} = 567$ nm) and emission spectrum ($\lambda_{ex} = 395$ nm) of TiO₂:Sm³⁺ NCs with different Sm³⁺ doping concentrations, and schematic energy-level diagrams to show the details of down-conversion mechanisms *via* excitation using 395 nm radiation for TiO₂:Sm³⁺ NCs. Adapted with permission.²⁴⁴ Copyright 2016, Elsevier.

overall efficiency of the present PV/T collector is 34.2%, with a 17.9% improvement. In a concentrator photovoltaic nanocrystal-phase change material (PCM) hybrid system, Al_2O_3 , CuO, and SiO_2 were used to save energy and offer safe operating conditions. Compared with pure PCM (0 wt%), Al_2O_3 -PCM at 5 wt% increased the thermal conductivity, and the melting rate reduced the solar cell temperature. The electrical efficiency was improved from 6.36% to 8% and gained temperature uniformity from 20 °C to 12 °C. This strategy would be recommended for residential and industrial applications in solar cells. Property in the present of the pres

4.6 Other functions

ZnSTe NCs with an average of 2.96 nm in the active layer demonstrated increased photo-generation and improved efficiency by reduced series resistance and improved mobility. Fe-doped SnO₂ NCs incorporated into the active layer of P3HT:PCBM improved the $J_{\rm sc}$ of OSC due to the extension of photogenerated exciton lifetime as a result of the magnetic field. Meanwhile, these NC-reinforced devices showed the tendency to overcome the burn-in regime faster and indicated the diluted magnetic semiconductor NCs had the potential to increase the stability of the devices. Fernill 1.20 and 1.20 are residued in the devices of the devices and indicated the diluted magnetic semiconductor NCs had the potential to increase the stability of the devices.

5. Summary and outlook

In recent years, NCs as functional layers and additives have been widely used in solar cells, significantly enhancing their performance. Here, we summarize NCs-based HTL, ETL, IFL, and additives for solar cells. NCs can boost the device performance in many ways, such as increasing the charge transport ability, suppressing charge recombination, broadening light harvest, and so on.

Based on previous investigations, we propose some promising strategies to enhance the performance of solar cells by using NCs.

- (I) Optical management. Full spectrum absorption under low-cost conditions: both up-converting and down-shifting materials. For down-shifting, doped NCs with large Stokes shift, such as Mn or Cu doped NCs, have great potential due to no self-absorption, facile synthesis, and low cost. Cu⁺, Ag⁺ doped n-type metal oxide NCs,²⁶⁰ Fe_{1-x}S₂ NCs,²⁶¹ and In doped CuxS NCs,²⁶² with great potential for spectra broadening are also suggested for high-performance solar cells. CaMoO₄:Er³⁺,Yb³⁺ NCs would offer great potential for conserving energy in Si solar cells.²⁶³ Certainly, the photoluminescence efficiency of NCs is very important when they are used to convert light in solar cells. Excellent optical management of solar cells can utilize more sunlight and improve the device performance.
- (II) Electronic optimization. The charge transfer ability is mainly determined by the electronic properties of charge transport materials. The performance of solar cells can be improved by electronic optimization. One approach is a component change of materials such as n doping for n-type NCs and p doping for p-type NCs. Finding more suitable dopants for NCs will further boost the PCE and stability of solar

Review Nanoscale Advances

cells. Meanwhile, the size and ligand control of NCs are also considered to optimize their electronic properties and fabricate better-performance solar cells.

(III) Interface engineering. Interfacial layers between different functional layers show different functions in solar cells. In further developments, more NCs IFL will be used to improve device performance by preventing direct contact between the active layer and charge transport layer, impeding the entry of water and oxygen, and protecting and destroying the active layer with UV lights.264 So, NC IFL, with good photoelectronic properties, can adjust energy alignment, accelerate charge transport, enhance light harvest, and protect the active laver.

(IV) Cross utilization. The metal-organic framework (MOF) materials can improve the efficiency and stability of solar cells due to their unique properties.265 NCs with small sizes can be considered to mix with MOF and enhance the performance of devices. In addition, NCs can be utilized as light harvesters, HTL, ETL, and IFL, so we suggest their application in all-NC solar cells.

Conflicts of interest

The authors declare no conflict of interest.

Acknowledgements

This work was supported by the Natural Science Foundation of the Guizhou Province (No. 2071). The authors thank Prof. Ma Wanli, Liu Zeke, and Dr Lu Huiyuan at Soochow University for their helpful discussion and suggestions for improving the manuscript.

References

- 1 I. J. Kramer and E. H. Sargent, The architecture of colloidal quantum dot solar cells: Materials to devices, Chem. Rev., 2014, 114, 863.
- 2 G. H. Carey, A. L. Abdelhady, Z. Ning, S. M. Thon, O. M. Bakr and E. H. Sargent, Colloidal quantum dot solar cells, Chem. Rev., 2015, 115, 12732.
- 3 K. R. Ryan, M. P. Down, N. J. Hurst, E. M. Keefe and C. E. Banks, Additive manufacturing (3D printing) of polymer electrically conductive polymers and nanocomposites and their applications, eScience, 2022, 2, 365-381.
- 4 M. J. Yuan, M. X. Liu and E. H. Sargent, Colloidal quantum dot solids for solution-processed solar cells, Nat. Energy, 2016, 1, 16016.
- 5 J. H. Jing, Y. J. Dou, S. H. Chen, K. Zhang and F. Huang, Solution sequential deposited organic photovoltaics: From morphology control to large-area modules, eScience, 2023, 3, 100142.
- 6 Z. K. Liu, J. Y. Yuan, S. A. Hawks, G. Z. Shi, S.-T. Lee and W. L. Ma, Photovoltaic devices based on colloidal PbX quantum dots: Progress and prospects, Sol. RRL, 2017, 1, 1600021.

7 Z. X. Pan, H. S. Rao, I. Mora-Seró, J. Bisquert and X. H. Zhong, Quantum dot-sensitized solar cells, Chem. Soc. Rev., 2018, 47, 7659-7702.

- 8 S. Aftab, M. Z. Igbal, S. Hussain, F. Kabir, A. A. Al-Kahtani and H. H. Hegazy, Quantum junction solar cells: Development and prospects, Adv. Funct. Mater., 2023, 33, 2303449.
- 9 A. Shrestha, M. Batmukh, A. Tricoli, S. Qiao and S. Dai, Near-infrared active lead chalcogenide quantum dots: post-synthesis ligand exchange, applications in solar cells, Angew. Chem., Int. Ed., 2019, 58, 5202-5224.
- 10 A. O. El-Ballouli, O. M. Bakr and O. F. Mohammed, Compositional, processing, and interfacial engineering of nanocrystal-and quantum-dot-based perovskite solar cells, Chem. Mater., 2019, 31, 6387-6411.
- 11 G. S. Selopal, H. Zhao, Z. M. Wang and F. Rosei, Core/shell quantum dots solar cells, Adv. Funct. Mater., 2020, 30, 1908762.
- 12 J. Y. Yuan, A. Hazarika, Q. Zhao, X. F. Ling, T. Moot, W. L. Ma and J. M. Luther, Metal halide perovskite in quantum dot solar cells: Progress and prospect, Joule, 2020, 4, 1160-1185.
- 13 F. G. Zhou, Z. Z. Li, H. Y. Chen, Q. Wang, L. M. Ding and Z. W. Jin, Application of perovskite nanocrystals (NCs)/ quantum dots (QDs) in solar cells, Nano Energy, 2020, 73, 104757.
- 14 M. Albaladejo-Siguan, E. C. Baird, D. Becker-Koch, Y. X. Li, A. L. Rogach and Y. Vaynzof, Stability of quantum dots solar cells: A matter of (life) time, Adv. Energy Mater., 2021, 11, 2003457.
- 15 J. W. Liu, K. H. Xian, L. Ye and Z. H. Zhou, Open-circuit voltage loss in lead chalcogenide quantum dot solar cell, Adv. Mater., 2021, 33, 2008115.
- 16 S. Liang, M. Y. Zhang, M. Biesold, W. Choi, Y. J. He, Z. L. Li, D. F. Shen and Z. Q. Lin, Recent advances in synthesis, properties, and applications of metal halide perovskite nanocrystals/polymer nanocomposites, Adv. Mater., 2021, 33, 2005888.
- 17 T. Kim, S. Lim, S. Yun, S. Jeong, T. Park and J. Choi, Design strategy of quantum dot thin-film solar cells, Small, 2020, 16, 2002460.
- 18 T. Blachowicz and A. Ehrmann, Recent development of solar cells from PbS colloidal quantum dots, Appl. Sci., 2020, 10, 1743.
- 19 Y. Liu, G. Z. Shi, Z. K. Liu and W. L. Ma, Toward printable solar cells based on PbX colloidal quantum dot inks, Nanoscale Horiz., 2021, 6, 8-23.
- 20 Y. Liu, F. Li, G. Z. Shi, Z. K. Liu, X. F. Lin, Y. Shi, Y. F. Chen, X. Meng, Y. Lv, W. Deng, X. Q. Pan and W. L. Ma, PbSe quantum dot solar cells based on directly synthesized semiconductive inks, ACS Energy Lett., 2020, 5, 3797-3803.
- 21 Y. Li, F. Yang, Y. J. Wang, G. Z. Shi, Y. M. Maung, J. Y. Yuan, S. J. Huang and W. L. Ma, Magnetron sputtered SnO₂ constituting double electron transport layers for efficient PbS quantum dot solar cells, Sol. RRL, 2020, 4, 2000218.

22 Y. N. Zhang, Y. Y. Kan, K. Gao, M. F. Gu, Y. Shi, X. L. Zhang, Y. Xue, X. N. Zhang, Z. K. Liu, Y. Zhang, J. Y. Yuan, W. L. Ma and A. K.-Y. Jen, Hybrid quantum dot/organic heterojunction: A route to improve open-circuit voltage in PbS colloidal quantum dot solar cells, *ACS Energy Lett.*,

Nanoscale Advances

2020, 5, 2335-2342.

- 23 J. Khan, X. L. Zhang, J. Y. Yuan, Y. Wang, G. Z. Shi, R. Patterson, J. W. Shi, X. F. Ling, L. Hu, T. Wu, S. Y. Dai and W. L. Ma, Tuning the surface-passivating ligand anchoring position enables phase robustness in CsPbI₃ perovskite quantum dot solar cells, *ACS Energy Lett.*, 2020, 5, 3322–3329.
- 24 X. F. Ling, J. Y. Yuan, X. L. Zhang, Y. L. Qian, S. M. Zakeeruddin, B. W. Larson, Q. Zhao, J. W. Shi, J. C. Yang, K. Ji, Y. N. Zhang, Y. J. Wang, C. Y. Zhang, S. Duhm, J. M. Luther, M. Grätzel and W. L. Ma, Guanidinium-assisted surface matrix engineering for highly efficient perovskite quantum dot photovoltaics, Adv. Mater., 2020, 32, 2001906.
- 25 K. Ji, J. B. Yuan, F. C. Li, Y. Shi, X. F. Ling, X. L. Zhang, Y. N. Zhang, H. Y. Lu, J. Y. Yuan and W. L. Ma, Highefficiency perovskite quantum dot solar cells benefiting from a conjugated polymer-quantum dot bulk heterojunction connecting layer, *J. Mater. Chem. A*, 2020, 8, 8104–8112.
- 26 X. L. Zhang, Y. L. Qian, X. F. Ling, Y. Wang, Y. N. Zhang, J. W. Shi, Y. Shi, J. Y. Yuan and W. L. Ma, α-CsPbBr3 perovskite quantum dots for application in semitransparent photovoltaics, *ACS Appl. Mater. Interfaces*, 2020, **12**, 27307–27315.
- 27 S. Lim, J. Kim, J. Y. Park, J. Min, S. Yun, T. Park, Y. Kim and J. Choi, Suppressed degradation and enhanced performance of CsPbI₃ perovskite quantum dot solar cells via engineering of electron transport layers, *ACS Appl. Mater. Interfaces*, 2021, **13**, 6119–6129.
- 28 S. Manzhos, C. C. Chueh, G. Giorgi, T. Kubo, G. Saianand, J. Lüder and M. Ihara, Materials design and optimization for next-generation solar cell and light-emitting technologies, J. Phys. Chem. Lett., 2021, 12, 4638–4657.
- 29 Y. Li, J. Zhu, Y. Huang, J. F. Wei, F. Liu, Z. P. Shao, L. H. Hu, S. H. Chen, S. F. Yang, J. W. Tang, J. X. Yao and S. Y. Dai, Efficient inorganic solid solar cells composed of perovskite and PbS quantum dots, *Nanoscale*, 2015, 7, 9902–9907.
- 30 J. Choi, Y. Kim, J. W. Jo, J. Kim, B. Sun, G. Walters, F. P. García de Arquer, R. Quintero-Bermudez, Y. Li, C. S. Tan, L. N. Quan, A. P. T. Kam, S. Hoogland, Z. H. Lu, O. Voznyy and E. H. Sargent, Chloride passivation of ZnO electrodes improves charge extraction in colloidal quantum dot photovoltaics, *Adv. Mater.*, 2017, 29, 1702350.
- 31 J. C. An, X. C. Yang, W. H. Wang, J. J. Li, H. X. Wang, Z. Yu, C. H. Gong, X. N. Wang and L. C. Sun, Stable and efficient PbS colloidal quantum dot solar cells incorporating low-temperature processed carbon paste counter electrodes, *Sol. Energy*, 2017, 158, 28–33.

- 32 X. L. Zhang, P. K. Santra, L. Tian, M. B. Johansson, H. Rensmo and E. M. J. Johansson, Highly efficient flexible quantum dot solar cells with improved electron extraction using MgZnO nanocrystals, *ACS Nano*, 2017, 11, 8478–8487.
- 33 J. Yang, J. Lee, J. Lee and W. Yi, Oxygen annealing of the ZnO nanoparticle layer for the high-performance PbS colloidal quantum-dot photovoltaics, *J. Power Sources*, 2019, 421, 124–131.
- 34 C. Mahajan, A. Sharma and A. K. Rath, Solution-phase hybrid passivation for efficient infrared-band gap quantum dot solar cells, *ACS Appl. Mater. Interfaces*, 2020, 12, 49840–49848.
- 35 Y. Y. Wei, M. B. Xing, D. D. Wang and R. X. Wang, Current density improvement of colloidal PbS quantum dot solar cells by adding NaCl in ZnO electron transport layer, *Energy Rep.*, 2020, **6**, 2370–2375.
- 36 M. B. Xing, Y. Y. Wei, D. D. Wang, Q. Shen and R. X. Wang, Mg-doped ZnO layer to enhance electron transporting for PbS quantum dot solar cells, *Curr. Appl Phys.*, 2021, 21, 14–19.
- 37 M. Biondi, M.-J. Choi, S. Lee, K. Bertens, M. Y. Wei, A. R. Kirmani, G. Lee, H. T. Kung, L. J. Richter, S. Hoogland, Z.-H. Lu, F. P. García de Arquer and E. H. Sargent, Control over ligand exchange reactivity in hole transport layer enables high-efficiency colloidal quantum dot solar cells, ACS Energy Lett., 2021, 6, 468–476.
- 38 S. Q. Liu, L. Hu, S. J. Huang, W. Q. Zhang, J. J. Ma, J. C. Wang, X. W. Guan, C.-H. Lin, J. Kim, T. Wan, Q. Lei, D. W. Chu and T. Wu, Enhancing the efficiency and stability of PbS quantum dot solar cells through engineering an ultrathin NiO nanocrystalline interlayer, ACS Appl. Mater. Interfaces, 2020, 12, 46239–46246.
- 39 M.-J. Choi, F. P. García de Arquer, A. H. Proppe, A. Seifitokaldani, J. Choi, J. Kim, S.-W. Baek, M. X. Liu, B. Sun, M. Biondi, B. Scheffel, G. Walters, D.-H. Nam, J. W. Jo, O. Ouellette, O. Voznyy, S. Hoogland, S. O. Kelley, Y. S. Jung and E. H. Sargent, Cascade surface modification of colloidal quantum dot inks enables efficient bulk homojunction photovoltaics, *Nat. Commun.*, 2020, 11, 103.
- 40 A. Sharma, N. V. Dambhare, J. Bera, S. Sahu and A. K. Rath, Crack-free conjugated PbS quantum dot-hole transport layers for solar cells, ACS Appl. Nano Mater., 2021, 4, 4016–4025.
- 41 M. Biondi, M.-J. Choi, O. Ouellette, S.-W. Baek, P. Todorović, B. Sun, S. Lee, M. Y. Wei, P. C. Li, A. R. Kirmani, L. K. Sagar, L. J. Richter, S. Hoogland, Z.-H. Lu, F. P. García de Arquer and E. H. Sargent, A chemically orthogonal hole transport layer for efficient colloidal quantum dot solar cells, *Adv. Mater.*, 2020, 32, 1906199.
- 42 Z. L. Teh, L. Hu, Z. L. Zhang, A. R. Gentle, Z. H. Chen, Y. J. Gao, L. Yuan, Y. C. Hu, T. Wu, R. J. Patterson and S. J. Huang, Enhanced power conversion efficiency via hybrid ligand exchange treatment of p-type PbS quantum dots, ACS Appl. Mater. Interfaces, 2020, 12, 22751–22759.

43 H. B. Wang, M. Desbordes, Y. Xiao, T. Kubo, T. Bessho, J. Nakazaki and H. Segawa, Highly stable interdigitated PbS quantum dot and ZnO nanowire solar cells with an automatically embedded electron-blocking layer, ACS Appl. Energy Mater., 2021, 4, 5918–5926.

- 44 G. Z. Shi, H. B. Wang, Y. H. Zhang, C. Cheng, T. S. Zhai, B. T. Chen, X. Y. Liu, R. Jono, X. N. Mao, Y. Liu, X. L. Zhang, X. F. Ling, Y. N. Zhang, X. Meng, Y. F. Chen, S. Duhm, L. Zhang, T. Li, L. Wang, S. Y. Xiong, T. Sagawa, T. Kubo, H. Segawa, Q. Shen, Z. K. Liu and W. L. Ma, The effect of water on colloidal quantum solar cells, *Nat. Commun.*, 2021, 12, 4381.
- 45 X. K. Yang, J. Yang, M. I. Ullah, Y. Xia, G. J. Liang, S. Wang, J. B. Zhang, H.-Y. Su, H. S. Song and J. Tang, Enhanced passivation and carrier collection in ink-processed PbS quantum dot solar cells via a supplementary ligand strategy, *ACS Appl. Mater. Interfaces*, 2020, **12**, 42217–42225.
- 46 K. Bertens, J. Z. Fan, M. Biondi, A. S. Rasouli, S. Leee, P. C. Li, B. Sun, S. Hoogland, F. P. García de Arquer, Z.-H. Lu and E. H. Sargent, Colloidal quantum dot solar cell band alignment using two-step ionic doping, ACS Mater. Lett., 2020, 2, 1583–1589.
- 47 D. Becker-Koch, M. Albaladejo-Siguan, Y. J. Hofstetter, O. Solomeshch, D. Pohl, B. Rellinghaus, N. Tessler and Y. Vaynzof, Doped organic hole extraction layers in efficient PbS and AgBiS₂ quantum dot solar cells, ACS Appl. Mater. Interfaces, 2021, 12, 18750–18757.
- 48 A. Chiu, E. Rong, C. Bambini, Y. D. Lin, C. C. F. Lu and S. M. Thon, Sulfur-infused hole transport materials to overcome performance-limiting transport in colloidal quantum dot solar cells, *ACS Energy Lett.*, 2020, 5, 2897–2904.
- 49 O. Ouellette, A. Lesage-Landry, B. Scheffel, S. Hoogland, F. P. García de Arquer and E. H. Sargent, Spatial collection in colloidal quantum dot solar cell, *Adv. Funct. Mater.*, 2020, 30, 1908200.
- 50 L. Hu, Q. Lei, X. W. Guan, R. Patterson, J. Y. Yuan, C.-H. Lin, J. Kim, X. Geng, A. Younis, X. X. Wu, X. F. Liu, T. Wan, D. W. Chu, T. Wu and S. J. Huang, Optimizing surface chemistry of PbS colloidal quantum dot for highly efficient and stable solar cells via chemical binding, *Adv. Sci.*, 2021, 8, 2003138.
- 51 L. Hu, X. Geng, S. Singh, J. J. Shi, Y. C. Hu, S. Y. Li, X. W. Guan, T. Y. He, X. N. Li, Z. X. Cheng, R. Patterson, S. J. Huang and T. Wu, Synergistic effect of electron transport layer and colloidal quantum dot solid enable PbSe quantum dot solar cell achieving over 10% efficiency, *Nano Energy*, 2019, 64, 103922.
- 52 M. H. Zhu, X. X. Liu, S. S. Liu, C. Chen, J. G. He, W. W. Liu, J. Yang, L. Gao, G. D. Niu, J. Tang and J. B. Zhang, Efficient PbSe colloidal quantum dot solar cells using SnO₂ as a buffer layer, *ACS Appl. Mater. Interfaces*, 2019, **12**, 2566–2571.
- 53 M. Albaladejo-Siguan, D. Becker-Koch, A. D. Taylor, Q. Sun, V. Lami, P. G. Oppennheimer, F. Paulus and Y. Vaynzof, Efficient and stable PbS quantum dot solar cells by triplecation perovskite passivation, ACS Nano, 2020, 14, 384–393.

- 54 A. R. Kirmani, F. García de Arquer, J. Z. Fan, J. I. Khan, G. Walters, S. Hoogland, N. Wehbe, M. M. Said, S. Barlow, F. Laquai, S. R. Marder, E. H. Sargent and A. Amassian, Molecular doping of the hole-transporting layer for efficient, single-step-deposited colloidal quantum dot photovoltaics, ACS Energy Lett., 2017, 2, 1952–1959.
- 55 C. Chen, L. Wang, L. Gao, D. Nam, D. B. Li, K. H. Li, Y. Zhao, C. Ge, H. Cheong, H. Liu, H. S. Song and J. Tang, 6.5% certified efficiency Sb₂Se₃ solar cells using PbS colloidal quantum dot film as hole-transporting layer, *ACS Energy Lett.*, 2017, 2, 2125–2132.
- 56 J. Choi, M.-J. Choi, J. Kim, F. Dinic, P. Todorovic, B. Sun, M. Y. Wei, S. Hoogland, F. P. García de Arquer, O. Voznyy and E. H. Sargent, Stabilizing surface passivation enables stable operation of colloidal quantum dot photovoltaic devices at maximum power point in an air ambient, *Adv. Mater.*, 2020, 32, 1906497.
- 57 M. Lv, J. Zhu, Y. Huang, Y. Li, Z. P. Shao, Y. F. Xu and S. Y. Dai, Colloidal CuInS₂ quantum dot as inorganic hole-transporting material in perovskite solar cells, *ACS Appl. Mater. Interfaces*, 2015, 7, 17482–17488.
- 58 Q. H. Li, J. K. Bai, T. T. Zhang, C. Nie, J. L. Duan and Q. W. Tang, CdZnSe@ZnSe colloidal alloy quantum dots for high-efficiency all-inorganic perovskite solar cells, *Chem. Commun.*, 2018, 54, 9575–9578.
- 59 M. Yuan, X. M. Zhang, J. Kong, W. H. Zhou, Z. J. Zhou, Q. W. Tian, Y. N. Meng, S. X. Wu and D. X. Kou, Controlling the band gap to improve open-circuit voltage in metal chalcogenide based perovskite solar cells, *Electrochim. Acta*, 2016, 215, 374–379.
- 60 Y. Li, Z. W. Wang, D. Ren, Y. H. Liu, A. B. Zheng, S. M. Zakeeruddin, X. D. Dong, A. Hagfeldt, M. Grätzel and P. Wang, SnS quantum dots as hole transporter of perovskite solar cells, ACS Appl. Energy Mater., 2019, 2, 3822–3829.
- 61 Y. Zhang, Z. L. Zhang, Y. Y. Liu, Y. F. Liu, H. P. Gao and Y. L. Mao, An inorganic hole-transport material of CuInSe₂ for stable and efficient perovskite solar cells, *Org. Electron.*, 2019, 67, 168–174.
- 62 F. Li, J. H. Wei, G. Q. Liao, C. Y. Guo, Y. Huang, Q. Zhang, X. Jin, S. Q. Jiang, Q. W. Tang and Q. H. Li, Quaternary quantum dots with gradient valence band for all-inorganic perovskite solar cells, *J. Colloid Interface Sci.*, 2019, 549, 33–41.
- 63 Y. L. Liu, X. Z. Zhao, Z. F. Yang, Q. T. Li, W. Wei, B. Hu and W. Chen, Cu₁₂Sb₄S₁₃ quantum dots with ligand exchanges as hole transport materials in all-inorganic perovskite CsPbI₃ quantum dot solar cells, *ACS Appl. Energy Mater.*, 2020, 3, 3521–3529.
- 64 M. Hedariramsheh, M. Mirhosseini, K. Abdizadeh, S. M. Mahdavi and N. Taghavinia, Evaluating Cu₂SnS₃ nanoparticle layers as hole-transporting materials in perovskite solar cells, ACS Appl. Energy Mater., 2021, 4, 5560–5573.
- 65 W. B. Ma, Z. L. Zhang, M. G. Ma, Y. F. Liu, G. C. Pan, H. P. Gao and Y. L. Mao, CuGaS₂ quantum dots with controlled surface defects as an hole-transport material

Nanoscale Advances

- for high-efficient and stable perovskite solar cells, Sol. Energy, 2020, 211, 55-61.
- 66 Y. Y. Liu, Z. L. Zhang, H. P. Gao, H. F. Zhang and Y. L. Mao, A novel inorganic hole-transporting material of CuInS₂ for perovskite solar cells with high efficiency and improved stability, Org. Electron., 2019, 75, 105430.
- 67 A. Kotta and H. K. Seo, Nickel oxide monodispersed quantum dots as hole transport layer in n-i-p hybrid perovskite solar cells, J. Nanoelectron. Optoelectron., 2019, 14, 895-899.
- 68 K. C. Icli and M. Ozenbas, Fully metal oxide charge selective layers for n-i-p perovskite solar cells employing nickel oxide nanoparticles, Electrochim. Acta, 2018, 263, 338-345.
- 69 S. Chakrabarti, D. Carolan, B. Alessi, P. Maguire, V. Svrcek and D. Mariotti, Microplasma-synthesized ultra-small NiO nanocrystals, a ubiquitous hole transport material, Nanoscale Adv., 2019, 1, 4915-4925.
- 70 K. Im, J. H. Heo, S. H. Im and J. Kim, Scalable synthesis of Ti-doped MoO₂ nanoparticle-hole-transporting-material with high moisture stability for CH₃NH₃PbI₃ perovskite solar cells, Chem. Eng. J., 2017, 330, 698-705.
- 71 A. Bashir, S. Shukla, J. H. Lew, S. Shukl, A. Bruno, D. Gupta, T. Baikie, R. Patidar, Z. Akhter, A. Priyadarshi, N. Mathews and S. G. Mhaisalkar, Spinel Co₃O₄ nanomaterials for efficient an stable large area cabon-based printed perovskite solar cells, Nanoscale, 2018, 10, 2341-2350.
- 72 C. Liu, X. Y. Zhou, S. M. Chen, X. Z. Zhao, S. Y. Dai and B. M. Xu, Hydrophobic Cu₂O quantum dots enabled by surfactant modification as top hole-transport materials for efficient perovskite solar cells, Adv. Sci., 2019, 6, 1801169.
- 73 S. Akin, Y. Liu, M. I. Dar, S. M. Zakeeruddin, M. Grätzel, S. Turan and S. Sonmezoglu, Hydrothermally processed CuCrO2 nanoparticles as an inorganic hole transporting material for low-cost perovskite solar cells with superior stability, J. Mater. Chem. A, 2018, 6, 20327-20337.
- 74 H. Zhang, H. Wang, W. Chen and A. K.-Y. Jen, CuGaO₂: A promising inorganic hole-transporting material for highly efficient and stable perovskite solar cells, Adv. Mater., 2017, 29, 1604984.
- 75 T.-C. Liang, H.-Y. Su, S.-A. Chen, Y.-J. Chen, C.-Y. Chiang, C.-H. Chiang, T.-T. Kao, L.-C. Chen and C.-C. Lin, Planar perovskite solar cells using perovskite CsPbI3 quantum dots as efficient hole transporting layers, Materials, 2022, 24, 8902.
- 76 L. Hu, W. W. Wang, H. Liu, J. Peng, H. F. Cao, G. Shao, Z. Xia, W. L. Ma and J. Tang, PbS colloidal quantum dots as an effective hole transporter for planar heterojunction perovskite solar cells, J. Mater. Chem. A, 2015, 3, 515-518.
- 77 L. S. Khanzada, I. Levchuk, Y. Hou, H. Azimi, A. Osvet, R. Ahmad, M. Brandl, P. Herre, M. Distaso, R. Hock, W. Peukert, M. Batentschuk and C. J. Brabec, Effective ligand engineering of the Cu₂ZnSnS₄ nanocrystal surface for increasing hole transport efficiency in perovskite solar cells, Adv. Funct. Mater., 2016, 26, 8300-8306.
- 78 G. Y. Ashebir, C. Dong, Z. Y. Wan, J. J. Qi, J. W. Chen, Q. Y. Zhao, W. W. Chen and M. T. Wang, Solution-

- processed Cu2ZnSnS4 nanoparticle film as efficient hole transporting layer for stable perovskite solar cells, *J. Phys.* Chem. Solids, 2019, 129, 204-208.
- 79 W. Lee, I. Kim, H. Choi and K. Kim, Synthesis of Ni/NiO core-shell nanoparticles for wet-coated hole transport layer of the organic solar cell, Surf. Coat. Technol., 2013, 231, 93-97.
- 80 S. S. Chen, S. W. Yang, H. Sun, L. Zhang, J. J. Peng, Z. Q. Liang and Z.-S. Wang, Enhanced interfacial electron transfer of inverted perovskite solar cells by introduction of CoSe into the electron-transporting-layer, J. Power Sources, 2017, 353, 123-130.
- 81 S. Weber, T. Rath, J. Mangalam, B. Kunert, A. M. Coclite, M. Bauch, T. Dimopoulos and G. Trimmel, Investigation of NiO_x-hole transport layers in triple cation perovskite solar cells, J. Mater. Sci., 2018, 29, 1847-1855.
- 82 D. Saranin, T. Komaricheva, L. Luchnikov, D. S. Muratov, T. S. Le, Y. Karpov, P. Gostishchev, S. Yurchuk, D. Kuznetsov, S. Didenko and A. D. Carlo, Hysteresis-free perovskite solr cells with compact and nanoparticle NiO for indoor application, Sol. Energy Mater. Sol. Cells, 2021, 227, 111095.
- 83 G. Luo, Y. X. Zhang, Q. L. Zhu, Z. Q. An, P. Lv, J. H. Chen, Y. Q. Zhu, M. Hu, W. N. Li, K. Cao, Z. L. Ku, W. C. Huang, Y.-B. Cheng and J. F. Lu, Ruthenium complex optimized contact interfaces nanocrystals for efficient and stable perovskite solar cells, Sol. RRL, 2023, 2300890.
- 84 J. B. You, L. Meng, T.-B. Song, T.-F. Guo, Y. Yang, W.-H. Chang, Z. R. Hong, H. J. Chen, H. P. Zhou, Q. Chen, Y. S. Liu, N. D. Marco and Y. Yang, Improved air stability of perovskite solar cells via solution-processed metal oxide transport layers, Nat. Nanotechnol., 2016, 11, 75-81.
- 85 M. Najafi, F. D. Giacomo, D. Zhang, S. Shanmugam, Senes, W. Verhees, A. Hadipour, Y. Galagan, T. Aernouts, S. Veenstra and R. Andriessen, Highly efficient and stable flexible perovskite solar cells with metal oxides nanoparticle charge extraction layers, Small, 2018, 14, 1702775.
- 86 H. Zhang, J. Q. Cheng, F. Lin, H. X. He, J. Mao, K. S. Wong, A. K.-Y. Jen and W. C. H. Choy, Pinhole-free and surfacenanostructured NiOx film by room-temperature solution process for high-performance flexible perovskite solar cells with good stability and reproducibility, ACS Nano, 2016, 10, 1503-1511.
- 87 J. J. He, E. B. Bi, W. T. Tang, Y. B. Wang, Z. M. Zhou, X. D. Yang, H. Chen and L. Y. Han, Ligand-free, highly dispersed NiOx nanocrystal for efficient, stable, lowtemperature processable perovskite solar cells, Sol. RRL, 2018, 2, 1800004.
- 88 Q. Q. He, K. Yao, X. F. Wang, X. F. Xia, S. F. Leng and F. Li, Room-temperature and solution-processable Cu-doped nickel oxide nanoparticles for efficient hole-transport layers of flexible large-area perovskite solar cells, ACS Appl. Mater. Interfaces, 2017, 9, 41887-41897.

89 J. J. He, Y. R. Xiang, F. Zhang, J. R. Lian, R. Hu, P. J. Zeng, J. Song and J. L. Qu, Improvement of red light harvesting ability and open circuit voltage of Cu:NiO_x based p-i-n planar perovskite solar cells boosted by cysteine enhanced interface contact, *Nano Energy*, 2018, 45, 471.

- 90 D. Ouyang, J. W. Zheng, Z. F. Huang, L. Zhu and W. C. H. Choy, An efficacious multifunction codoping strategy on a room-temperature solution-processed hole transport layer for realizing high-performance perovskite solar cells, *J. Mater. Chem. A*, 2021, **9**, 371–379.
- 91 J. Wang, J. Zhang, Y. Z. Zhou, H. B. Liu, Q. F. Xue, X. S. Li, C.-C. Chueh, H.-L. Yip, Z. L. Zhu and A. K.-Y. Jen, Highly efficient all-inorganic perovskite solar cells with suppressed non-radiative recombination by a Lewis base, *Nat. Commun.*, 2020, **11**, 177.
- 92 A. Savva, I. T. Papadas, D. Tsikritzis, G. S. Armatas, S. Kennou and S. A. Choulis, Room temperature nanoparticulate interfacial layers for perovskite solar cells via solvothermal synthesis, *J. Mater. Chem. A*, 2017, 5, 2038120389.
- 93 W. A. Dunlap-Shohl, T. B. Daunis, X. M. Wang, J. Wang, B. Y. Zhang, D. Barrera, Y. F. Yan, J. W. P. Hsu and D. B. Mitzi, Room-temperature fabrication of a delafossite CuCrO₂ hole transport layer for perovskite solar cells, *J. Mater. Chem. A*, 2018, 6, 469–477.
- 94 H. Zhang, H. Wang, H. M. Zhu, C.-C. Chueh, W. Chen, S. H. Yang and A. K.-Y. Jen, Low-temperature solution-pocessed CuCrO₂ hole-transporting layer for efficient and photostable perovskite solar cells, *Adv. Energy Mater.*, 2018, **8**, 1702762.
- 95 I. T. Papadas, A. Savva, A. Loakeimidis, P. Eleftheriou, G. S. Armatas and S. A. Choulis, Employing surfactantassisted hydrothermal synthesis to control CuGaO₂ nanoparticle formation and improved carrier selectivity of perovskite solar cells, *Mater. Today Energy*, 2018, 8, 57–64.
- 96 D. Ouyang, J. Y. Xiao, F. Ye, Z. F. Huang, H. Zhang, L. Zhu, J. Q. Cheng and W. C. H. Choy, Strategic synthesis of ultrasmall NiCo₂O₄ NPs as hole transport layer for highly efficient perovskite solar cells, *Adv. Energy Mater.*, 2018, 16, 1702722.
- 97 I. T. Papadas, A. Ioakeimidis, G. S. Armatas and S. A. Choulis, Low-temperature combustion synthesis of a spinel NiCo₂O₄ hole transport layer for perovskite photovoltaics, *Adv. Sci.*, 2018, 5, 1701029.
- 98 Z. F. Huang, D. Ouyang, R. M. Ma, W. Wu, V. A. L. Roy and W. C. H. Choy, A general method: Designing a hypocrystalline hydroxide intermediate to achieve ultrasmall and well-dispersed ternary metal oxide for efficient photovoltaic devices, *Adv. Funct. Mater.*, 2019, 29, 1904684.
- 99 B. P. Yang, D. Ouyang, Z. F. Huang, X. G. Ren, H. Zhang and W. C. H. Choy, Multifunctional synthesis approach of In:CuCrO₂ nanopaticles for hole transport layer in highperformance perovskite solar cells, *Adv. Funct. Mater.*, 2019, 29, 1902600.
- 100 A. Kumar, D. K. Jarwal, A. K. Mishra, S. Ratan, C. Kumar, R. K. Upadhyay, B. Mukherjee and S. Jit, Effects of HTL

- and ETL thicknesses on the performance of PQT-12/PCDTBT:PC₆₁BM/ZnO QDs solar cells, *IEEE Photonics Technol. Lett.*, 2020, 32, 677–680.
- 101 B. P. Yang, S. M. Peng and W. C. H. Choy, Inorganic top electron transport layer for high performance inverted perovskite solar cells, *EcoMat*, 2021, 3, e12127.
- 102 A. Wibowo, M. A. Marsudi, M. I. Amal, M. B. Ananda, R. Stephanie, H. Ardy and L. J. Diguna, ZnO nanostructured materials for emerging solar cell applications, *RSC Adv.*, 2020, **10**, 42838–42859.
- 103 S. B. Shivarudraiah, M. Ng, C.-H. A. Li and J. E. Halpert, Allinorganic, solution-processed, inverted CsPbI₃ quantum dot solar cells with a PCE of 13.1% achieved via a layer-by-layer FAI treatment, ACS Appl. Energy Mater., 2020, 3, 5620–5627
- 104 L. J. Meng, Q. W. Xu, U. K. Thakur, L. Gong, H. B. Zeng, K. Shankar and X. H. Wang, Unusual surface ligand doping-induced p-type quantum dot slides and their application in solar cells, ACS Appl. Mater. Interfaces, 2020, 12, 53942–53949.
- 105 T. T. Jiang and W. F. Fu, Improved performance and stability of perovskite solar cells with bilayer electron-transporting layers, *RSC Adv.*, 2018, **8**, 5897–5901.
- 106 C.-J. Chen, A. Chandel, D. Thakur, J.-R. Wu, S.-E. Chiang, G.-S. Zeng, J.-L. Shen, S.-H. Chen and S. H. Chang, Ag modified bathocuproine:ZnO nanoparticles electron buffer layer based bifacial inverted-type perovskite solar cells, *Org. Electron.*, 2021, 92, 106110.
- 107 Y.-H. Chiang, C.-K. Shih, A.-S. Sie, M.-H. Li, C.-C. Peng, P.-S. Shen, Y.-P. Wang, T.-F. Guo and P. Chen, Highly stable perovskite solar cells with all-inorganic selective contacts from microwave-synthesized oxide nanoparticles, *J. Mater. Chem. A*, 2017, 5, 25485–25493.
- 108 P.-H. Lee, T.-T. Wu, K.-Y. Tian, C.-F. Li, C.-H. Hou, J.-J. Shyue, C.-F. Lu, Y.-C. Huang and W.-F. Su, Workfunction-tunable electron transport layer of molecule-capped metal oxide for a high-efficiency and stable p-in perovskite solar cells, ACS Appl. Mater. Interfaces, 2020, 12, 45936–45949.
- 109 Y. Zhao, H. Zhang, X. G. Ren, H. L. Zhu, Z. F. Huang, F. Ye, D. Ouyang, K. W. Cheah, A. K.-Y. Jen and W. C. H. Choy, Thick TiO₂-based top electron transport layer on perovskite for highly efficient and stable solar cells, *ACS Energy Lett.*, 2018, 3, 2891–2898.
- 110 S. S. Zhang, W. T. Chen, S. H. Wu, R. Chen, Z. H. Liu, Y. Q. Huang, Z. C. Yang, H. M. Zhu, J. Y. Li, L. Y. Han and W. Chen, Hybrid inorganic electron-transporting layer coupled with a halogen-resistant electrode in CsPbI₂Br-based perovskite solar cells to achieve robust long-term stability, *ACS Appl. Mater. Interfaces*, 2019, 11, 43303–43311.
- 111 J. Lim, W. Jang, M. S. Kim, M. Ji, Y.-I. Lee and D. H. Wang, Hydrogenerated black titanium dioxide-embedded conducting polymer for boosting electron flow in perovskite devices, *J. Alloys Compd.*, 2020, **846**, 156329.
- 112 R. Fang, S. H. Wu, W. T. Chen, Z. H. Liu, S. S. Zhang, R. Chen, Y. F. Yue, L. L. Deng, Y.-B. Cheng, L. Y. Han and

Nanoscale Advances Review

- W. Chen, [6,6]-Phenyl-C₆₁-butyric acid methyl ester/cerium oxide bilayer structure as efficient and stable electron transport layer for inverted perovskite solar cells, ACS Nano, 2018, 12, 2403-2414.
- 113 B. P. Yang, R. M. Ma, Z. S. Wang, D. Ouyang, Z. F. Huang, J. L. Lu, X. H. Duan, L. Yue, N. Xu and W. C. H. Choy, Efficient gradient potential top electron transport structures achieved by combining an oxide family for inverted perovskite solar cells with high efficiency and stability, ACS Appl. Mater. Interfaces, 2021, 13, 27179-27187.
- 114 F. R. Tan, W. Z. Xu, X. D. Hu, P. Yu and W. F. Zhang, Highly efficient inverted perovskite solar cells with CdSe QDs/LiF electron transporting layer, Nanoscale Res. Lett., 2017, 12, 614
- 115 R. T. Ako, P. Ekanavake, D. J. Young, J. Hobley, V. Chellappan, A. Tan, S. Gorelik, G. S. Subramanian and C. M. Lim, Evaluation of surface energy state distribution and bulk defect concentration in DSSC photoanodes based on Sn, Fe, and Cu doped TiO2, Appl. Surf. Sci., 2015, 351, 950-961.
- 116 M. Neetu, I. C. Maurya, A. K. Gupta, P. Srivastava and L. Bahadur, Extensive enhancement in power conversion efficiency of dye-sensitized solar cell by using Al-doped TiO₂ photoanode, J. Solid State Electrochem., 2017, 21, 1229-1241.
- 117 B. Ünlü, S. Cakar and M. Özacar, The effects of metal doped on DSSCs TiO₂ and dithizone-metal complexes performance, Sol. Energy, 2018, 166, 441-449.
- 118 J. Manju and S. J. Jawhar, Facile synthesis and characterization of Ti_(1-x)Cu_xO₂ nanoparticles for high efficiency dye sensitized solar cell applications, Opt. Mater., 2017, 69, 119-127.
- 119 M.-J. Lee, J.-Y. Park, C.-S. Kim, K. Okuyama, S.-E. Lee and T.-O. Kim, Improvement of light scattering capacity in dve-sensitized solar cells by doping with nanoparticles, J. Power Sources, 2016, 327, 96-103.
- 120 S. Kundu, P. Sarojinijeeva, R. Karthick, G. Anantharaj, G. Saritha, R. Bera, S. Anandan, A. Patra, P. Ragupathy, M. Selvaraj, D. Jeyakumar and K. Pillai, Enhancing the efficiency of DSSCs by the modification of TiO₂ photoanodes using N, F, and S, co-doped graphene quantum dots, Electrochim. Acta, 2017, 242, 337-343.
- 121 X. Z. Zhang, T. Y. Wu, X. X. Xu, L. Zhang, J. Tang, X. He, J. H. Wu and Z. Lan, Ligand-exchange TiO2 nanocrystals induced formation of high-quality electron transporting layers at low temperature for efficient planar perovskite solar cells, Sol. Energy Mater. Sol. Cells, 2018, 178, 65-73.
- Sanglee, S. Chuangcote, T. J. Sritharathikhun, K. Sriprapha and T. Sagawa, Quantum dot-modified titanium dioxide nanoparticles as an energyband tunable electron-transporting layer for open airfabricated planar perovskite solar cells, Nanomater. Nanotechnol., 2020, 10, 1847980420961638.
- 123 R. Singh, I. Ryu, H. Yadav, J. Park, J. W. Jo, S. Yim and J.-J. Lee, Non-hydrolytic sol-gel route to synthesize TiO₂ nanoparticles under ambient condition for highly

- efficient and stable perovskite solar cells, Sol. Energy, 2019, 185, 307-314.
- 124 A. Badawi, N. Al-Hosiny and S. Abdallah, The photovoltaic performance of CdS quantum dots sensitized solar cell using graphene/TiO2 working electrode, Superlattices Microstruct., 2015, 81, 88-96.
- 125 P. N. Kumar, R. Narayanan, S. Laha, M. Deepa and A. K. Srivastava, Phoroelectrochromic cell with a CdS quantum dots/graphitic-nanoparticles sensitized anode and a molybdenum oxide cathode, Sol. Energy Mater. Sol. Cells, 2016, 153, 138-147.
- 126 Z. Zolfaghari-Isavandi and Z. Shariatinia, Enhanced efficiency of quantum dot sensitized solar cells using Cu₂O/TiO₂ nanocomposite photoanodes, J. Alloys Compd., 2018, 737, 99-112.
- 127 S. Zhang, Z. Lan, J. H. Wu, X. Chen and C. Y. Zhang, Preparation of novel TiO@ quantum dot blocking layers at conductive glass/TiO2 interfaces for efficient CdS quantum dot sensitized solar cells, J. Alloys Compd., 2016, 656, 253-258.
- 128 M. Marandi, P. Talebi and S. Bayat, Optimization of the doping process and light scattering in CdS:Mn quantum dots sensitized solar cells for the efficiency enhancement, J. Mater. Sci.: Mater. Electron., 2019, 30, 3820-3832.
- 129 Y. B. Lu, L. Li, S. C. Su, Y. J. Chen, Y. L. Song and S. J. Jiao, A novel TiO₂ nanostructure as photoanode for highly efficient CdSe quantum dot-sensitized solar cells, RSC Adv., 2017, 7, 9795-9802.
- 130 J. P. Deng, M. Q. Wang, J. F. Fang, X. H. Song, Z. Yang and Z. L. Yuan, Synthesis of Zn-doped TiO₂ nano-particles using metal Ti and Zn as raw materials and application in quantum dot sensitized solar cells, J. Alloys Compd., 2019, **791**, 371-379.
- 131 S. M. Thon, A. H. Ip, O. Voznyy, L. Levina, K. W. Kemp, G. H. Carey, S. Masala and E. H. Sargent, Role of bond adaptability in the passivation of colloidal quantum dot solids, ACS Nano, 2013, 7, 7680-7688.
- 132 A. E. Tom, A. Thomas and V. V. Ison, Novel post-synthesis purification strategies and the ligand exchange processes in simplifying the fabrication of PbS quantum dot solar cells, RSC Adv., 2020, 10, 30707-30715.
- 133 N. L. Zhang, D. C. J. Neo, Y. Tazawa, X. T. Li, H. E. Assender, R. G. Compton and A. A. R. Watt, Narrow band gap lead hole transport layers for quantum dot photovoltaics, ACS Appl. Mater. Interfaces, 2016, 8, 21417-21422.
- 134 D. C. J. Neo, N. L. Zhang, Y. Tazawa, H. B. Jiang, G. M. Hughes, C. R. M. Grovenor, H. E. Assender and A. A. R. Watt, Poly(3-hexylthiophene-2,5-diyl) as a hole transport layer for colloidal quantum dot solar cells, ACS Appl. Mater. Interfaces, 2016, 8, 12101.
- 135 A. Mnoyan, K. Kim, J. Y. Kim and D. Y. Jeon, Colloidal nanocomposite of reduced grapheme oxide and quantum dots for enhanced surface passivation in optoelectronic applications, Sol. Energy Mater. Sol. Cells, 2016, 144, 181-186.

136 S. P. Zang, Y. L. Wang, M. Y. Li, W. Su, H. C. Zhu, X. T. Zhang and Y. C. Liu, Fabrication of efficient PbS colloidal quantum dot solar cell with low temperature sputter-deposited ZnO electron transport layer, *Sol. Energy Mater. Sol. Cells*, 2017, 169, 264–269.

- 137 J. Choi, J. W. Jo, F. P. García de Arquer, Y.-B. Zhao, B. Sun, J. Kim, M.-J. Choi, S.-W. Baek, A. H. Proppe, A. Seifitokaldani, D.-H. Nam, P. Li, O. Ouellette, Y. Kim, O. Voznyy, S. Hoogland, S. O. Kelley, Z.-H. Lu and E. H. Sargent, Activated electron-transport layers for infrared quantum dot optoelectronics, *Adv. Mater.*, 2018, 30, 1801720.
- 138 Y. Xue, F. Yang, J. Y. Yuan, Y. N. Zhang, M. F. Gu, Y. L. Xu, X. F. Ling, Y. Wang, F. C. Li, T. S. Zhai, J. N. Li, C. H. Cui, Y. W. Chen and W. L. Ma, Toward scalable PbS quantum dot solar cells using a tailored polymeric hole conductor, *ACS Energy Lett.*, 2019, 4, 2850–2858.
- 139 E. G. Durmusoglu, G. S. Selopal, M. Mohammadnezhad, H. Zhang, P. Dagtepe, D. Barba, S. H. Sun, H. G. Zhao, H. Y. Acar, Z. M. Wang and F. Rosei, Low-cost, airprocessed quantum dot solar cells via diffusion-controlled synthesis, ACS Appl. Mater. Interfaces, 2020, 12, 36301– 36310.
- 140 C. Ding, F. Liu, Y. H. Zhang, S. Hayase, T. Masuda, R. X. Wang, Y. Zhou, Y. F. Yao, Z. G. Zou and Q. Shen, Passivation strategy of reducing both electron and hole states for achieving high-efficiency PbS quantum-dot solar cells with power conversion efficiency over 12%, ACS Energy Lett., 2020, 5, 3224–3236.
- 141 T. S. Zhao, E. D. Goodwin, J. C. Guo, H. Wang, B. T. Diroll, C. B. Murray and C. R. Kagan, Advanced architecture for colloidal PbS quantum dot solar cells exploiting a CdSe quantum dot buffer layer, ACS Nano, 2016, 10, 9267–9273.
- 142 S. Kumar, R. Upadhyay and B. Pradhan, Performance enhancement of heterojunction ZnO/PbS quantum dot solar cells by interface engineering, *Sol. Energy*, 2020, **211**, 283–290.
- 143 J. P. Deng, M. Q. Wang, W. Ye, J. F. Fang, P. C. Zhang, Y. P. Yang and Z. Yang, CdS/CdSe-sensitized solar cell based on Al-doped ZnO nanoparticles prepared by the decomposition of zinc acetate solid solution, *Solid-State Electron.*, 2017, 127, 38–44.
- 144 F. Yang, Y. L. Xu, M. F. Gu, S. J. Zhou, Y. J. Wang, K. Y. Lu, Z. K. Liu, X. F. Ling, Z. J. Zhu, J. M. Chen, Z. Y. Wu, Y. N. Zhang, Y. Xue, F. C. Li, J. Y. Yuan and W. L. Ma, Synthesis of cesium-doped ZnO nanoparticles as an electron extraction layer for efficient PbS colloidal quantum dot solar cells, *J. Mater. Chem. A*, 2018, 6, 17688–17697.
- 145 N. Sukharevska, D. Bederak, V. M. Goossens, J. Momand, H. Duim, D. N. Dirin, M. V. Kovalenko, B. J. Kooi and M. A. Loi, Scalable PbS quantum dot solar cell production by blade coating from stable inks, ACS Appl. Mater. Interfaces, 2021, 13, 5195–5207.
- 146 X. S. Zhang, Z. W. Jin, J. R. Zhang, D. L. Bai, H. Bian, K. Wang, J. Sun, Q. Wang and S. Z. F. Liu, All-inorganic processed binary CsPbBr₃-CsPb₂Br₅ perovskites with

- synergistic enhancement for high-efficiency Cs-Pb-Br-based solar cells, *ACS Appl. Mater. Interfaces*, 2018, **10**, 7145–7154.
- 147 Y. N. Zhang, Y. Y. Kan, K. Gao, M. F. Gu, Y. Shi, X. L. Zhang, Y. Xue, X. N. Zhang, Z. K. Liu, Y. Zhang, J. Y. Yuan, W. L. Ma and A. K.-Y. Jen, Hybrid quantum dot/organic heterojunction: A route to improve open-circuit voltage in PbS colloidal quantum dot solar cells, *ACS Energy Lett.*, 2020, 5, 2335–2342.
- 148 P. D. Li, T. G. Jiu, G. Tang, G. J. Wang, J. Li, X. F. Li and J. F. Fang, Solvents induced ZnO nanoparticles aggregation associated with their interfacial effect on organic solar cells, ACS Appl. Mater. Interfaces, 2014, 6, 18172–18179.
- 149 S. Bishnoi, V. Gupta, C. Sharma, D. Haranath, M. Kumar and S. Chand, Luminescent cathode buffer layer for enhanced power conversion efficiency and stability of bulk-heterojunction solar cells, *Org. Electron.*, 2016, 38, 193–199.
- 150 M. Abrari, M. Ghanaatshoar, H. R. Moazami and S. S. H. Davarani, Synthesis of SnO2 nanoparticles by electrooxidation method and their application in dyesensitized solar cells: The influence of the counterion, *J. Electron. Mater.*, 2019, **48**, 445–453.
- 151 A. E. Shalan, M. Rasly, I. Osama, M. M. Rashad and I. A. Ibrahim, Photpcurrrent enhancement by Ni²⁺ and Zn²⁺ ion doped in SnO₂ nanoparticles in highly porous dye-sensitized solar cells, *Ceram. Int.*, 2014, 40, 11619– 11626.
- 152 Y. Wang, M. L. Feng, H. R. Chen, M. Ren, H. F. Wang, Y. F. Miao, Y. T. Chen and Y. X. Zhao, Highly crystalized Cl-doped SnO₂ nanocrystals for stable aqueous dispersion toward high-performance perovskite photovoltaics, *Adv. Mater.*, 2023, 23058498.
- 153 M. Saeidi, M. Abrari and M. Ahmadi, Fabrication of dyesensitized solar cell based on mixed tin and zinc oxide nanoparticles, *Appl. Phys. A*, 2019, **125**, 409.
- 154 M. Asemi and M. Ghanaatshoar, Studying the effect of the controlled off-stoichiometry on the properties of Zn₂SnO₄ nanoparticles for DSSC applications, *J. Mater. Sci.*, 2018, 29, 6730–6740.
- 155 A. P. S. Souza, F. G. S. Oliveira, V. F. Nunes, F. M. Lima, A. F. L. Almeida, I. M. M. de Carvalho and M. P. F. Graca, High performance SnO₂ pure photoelectrode in dyesensitized solar cells achieved via electrophoretic technique, *Sol. Energy*, 2020, 211, 312–323.
- 156 K. Balasubramanian and G. Venkatachari, Synthesis and characterization of Sb doped SnO₂ for the photovoltaic applications: different route, *Mater. Res. Express*, 2019, **6**, 1250k6.
- 157 S. J. In, M. Park and J. W. Jung, Reduced interface energy loss in non-fullerene organic solar cells using room temperature-synthesis SnO₂ quantum dots, *J. Mater. Sci. Technol.*, 2020, **52**, 12–19.
- 158 T. Y. Kong, R. Wang, D. Zheng and J. S. Yu, Modification of the SnO_2 electron transporting layer by using perylene

Nanoscale Advances

- diimide derivative for efficient organic solar cells, Front. Chem., 2021, 9, 703561.
- 159 S. Guang, J. Yu, H. Wang, X. Liu, S. Qu, R. Zhu and W. Tang, J. Energy Chem., 2021, 56, 496.
- 160 S. N. Vijayaraghavan, J. Wall, L. Li, G. Xing, Q. Zhang and F. Yan, Low-temperature processed highly efficient hole transport layer free carbon-based planar perovskite solar cells with SnO2 quantum dot electron transport layer, Mater. Today Phys., 2020, 13, 100204.
- 161 Z. Ma, W. Y. Zhou, Z. Xiao, H. Zhang, Z. Y. Li, J. Zhuang, C. T. Peng and Y. L. Huang, Negligible hysteresis planar perovskite solar cells using Ga-doped SnO2 nanocrystal as electron transport layers, Org. Electron., 2019, 71, 98-105.
- 162 S. Y. Park and H. C. Shim, Highly efficient and air-stable heterostructured perovskite quantum dot solar cells sing a solid-state cation-exchange reaction, ACS Appl. Mater. Interfaces, 2020, 12, 57124-57133.
- 163 M. Singh, A. Ng, Z. Ren, H. L. Hu, H.-C. Lin, C.-W. Chu and G. Li, Facile synthesis of composite tin oxide nanostructures for high-performance planar perovskite solar cells, Nano Energy, 2019, 60, 275-284.
- 164 H. X. Xie, X. T. Yin, P. Chen, J. Liu, C. H. Yang, W. X. Que and G. F. Wang, Solvothermal synthesis of highly crystalline SnO2 nanoparticles for flexible perovskite solar cells application, Mater. Lett., 2019, 234, 311-314.
- 165 Z. C. Wang, T. Wu, L. Xiao, P. L. Qin, X. L. Yu, L. Ma, L. Xiong, H. X. Li, X. B. Chen, Z. Wang, T. Wu, L. Xiao, P. Qin, X. Yu, L. Ma, L. Xiong, H. Li and X. Chen, potassium Multifunctional hexafluorophosphate passivates interface defects for high efficiency perovskite solar cells, J. Power Sources, 2021, 488, 229451.
- 166 H. R. Liu, Z. L. Chen, H. B. Wang, F. H. Ye, J. J. Ma, X. L. Zheng, P. B. Gui, L. B. Xiong, J. Wen and G. J. Fang, A facial room temperature solution synthesis of SnO2 quantum dots for perovskite solar cells, J. Mater. Chem. A, 2019, 7, 10636-10643.
- 167 G. Yang, C. Chen, F. Yao, Z. L. Chen, Q. Zhang, X. L. Zheng, J. J. Ma, H. W. Lei, P. L. Qin, L. B. Xiong, W. J. Ke, G. Li, Y. F. Yan and G. J. Fang, Effective carrier-concentration tuning of SnO2 quantum dot electron-selective layers for high-performance planar perovskite solar cells, Adv. Mater., 2018, 30, 1706023.
- 168 M. Kim, J. Jeong, H. Lu, T. K. Lee, F. T. Eickemeyer, Y. Liu, I. W. Choi, S. J. Choi, Y. Jo, H.-B. Kim, S.-I. Mo, Y.-K. Kim, H. Lee, N. G. An, S. Cho, W. R. Tress, S. M. Zakeeruddin, A. Hagfeldt, J. Y. Kim, M. Grätzel and D. S. Kim, Conformal quantum dot-SnO₂ layers as transporters for efficient perovskite solar cells, Science, 2022, 375, 302-306.
- 169 Y. Wang, C. H. Duan, X. L. Zhang, N. Rujisamphan, Y. Liu, Y. Y. Li, J. Y. Yuan and W. L. Ma, Dual interfacial engineering enables efficient and reproducible CsPbI2Br all-inorganic perovskite solar cells, ACS Appl. Mater. Interfaces, 2020, 12, 31659-31666.
- 170 R. X. Peng, T. T. Yan, J. W. Chen, S. F. Yang, Z. Y. Ge and M. T. Wang, Passivating surface defects of n-SnO₂ electron transporting layer by InP/ZnS quantum dots:

- Toward efficient and stable organic solar cells, Adv. Electron. Mater., 2020, 6, 1901245.
- 171 N. Huang, G. W. Li, H. Huang, P. P. Sun, T. L. Xiong, Z. F. Xia, F. Zheng, J. Xu and X. H. Sun, One-step solvothermal tailoring the compositions and phases of nickel cobalt sulfides on conducting oxide substrates as counter electrodes for efficient dye-sensitized solar cells, Appl. Surf. Sci., 2016, 390, 847-855.
- 172 K. Al-Attafi, F. H. Jawdat, H. Qutaish, P. Hayes, A. Al-Keisy, K. Shim, Y. Yamauchi, S. X. Dou, A. Nattestad and J. H. Kim, Cubic aggregates of Zn₂SnO₄ nanoperticles and their application in dye-sensitized solar cells, Nano Energy, 2019, 57, 202-213.
- 173 Q. Jiang, L. Zhang, H. Wang, X. Yang, J. Meng, H. Liu, Z. Yin, J. Wu, X. Zhang and J. You, Nat. Energy, 2017, 2, 16177.
- 174 H.-J. Kim, G.-C. Xu, C. V. V. M. Gopi, H. Seo, M. Venkata-Haritha and M. Shiratani, Enhanced light harvesting and charge recombination control with TiO2/PbCdS/CdS based quantum dot-sensitized solar cells, I. Electroanal. Chem., 2017, 788, 131-136.
- 175 E. Jalali-Moghadam and Z. Shariatinia, Al³⁺ doping into TiO2 photoanodes improved the performance of amine anchored CdS quantum dot sensitized solar cells, Mater. Res. Bull., 2018, 98, 121-132.
- 176 S. Muthu, G. Zaiats, M. B. Sridharan and P. V. Kamat, influence of plasmonic CuxS interfacing layer on photovoltaic performance of CIZS quantum dot sensitized solar cells, J. Electrochem. Soc., 2019, 166, H3133-H3137.
- 177 H. T. Dastjerdi, P. F. Qi, Z. Y. Fan and M. M. Tavakoli, Costeffective and semi-transparent PbS quantum dot solar cells using copper electrodes, ACS Appl. Mater. Interfaces, 2020, 12, 818-825.
- 178 Z. L. Zhang, Z. H. Chen, J. B. Zhang, W. J. Chen, J. F. Yang, X. M. Wen, B. Wang, N. Kobamoto, L. Yuan, J. A. Stride, G. J. Conibeer, R. J. Patterson and S. J. Huang, Significant improvement in the performance of PbSe quantum dot solar cell by introducing CsPbBr3 perovskite colloidal nanocrystal back layer, Adv. Energy Mater., 2017, 7, 1601773.
- 179 H. Ren, A. Xu, Y. Y. Pan, D. H. Qin, L. T. Hou and D. Wang, Efficient PbS quantum dot solar cells with both Mg-doped ZnO window layer and ZnO nanocrystal interface passivation layer, Nanomaterials, 2021, 11, 219.
- 180 K. M. Kim, J. H. Jeon, Y. Y. Kim, H. K. Lee, O. O. Park and D. H. Wang, Effects of ligand exchange CdSe quantum dot interlayer for inverted organic solar cells, Org. Electron., 2015, 25, 44-49.
- 181 Z. Q. Li, S. J. Li, Z. H. Zhang, X. Y. Zhang, J. F. Li, C. Y. Liu, L. Shen, W. B. Guo and S. P. Ruan, Enhanced electron extraction capability of polymer solar cells via modifying the cathode buffer layer with inorganic quantum dots, Phys. Chem. Chem. Phys., 2016, 18, 11435-11442.
- 182 J. H. Jeon, D. H. Wang, H. Park, J. H. Park and O. O. Park, Stamping transfer of a quantum dot interlayer for organic photovoltaic cells, Langmuir, 2012, 28, 9893-9898.
- 183 C. H. Duan, W. N. Luo, T. G. Jiu, J. S. Li, Y. Wang and F. S. Lu, Facile preparation and characterization of ZnCdS

nanocrystals for interfacial applications in photovoltaic devices, *J. Colloid Interface Sci.*, 2018, **512**, 353–360.

- 184 S. Huang, Y. T. Tang, A. C. Yu, Y. H. Wang, S. Shen, B. N. Kang, S. R. P. Silva and G. Y. Lu, Solution-processed SnO₂ nanoparticle interfacial layers for efficient electron transport in ZnO-based polymer solar cells, *Org. Electron.*, 2018, 62, 373–381.
- 185 M. Dusza, M. Stefanski, M. Wozniak, D. Hreniak, Y. Gerasymchuk, L. Marciniak, F. Granek and W. Strek, Luminescent Sr₂CeO₄ nanocrystals for applications in organic solar cells with conjugated polymers, *J. Lumin.*, 2016, 169, 857–861.
- 186 Z. Zhang, Y. Yang, J. Gao, S. Xiao, C. H. Zhou, D. Q. Pan, G. Liu and X. Y. Guo, Highly efficient Ag₂Se quantum dots blocking layer for solid-state dye-sensitized solar cells: Size effects on device performance, Mater, *Mater. Today Energy*, 2018, 7, 27–36.
- 187 S. S. Hosseini, M. Ebadi and K. Motevalli, Facial microwave approach for synthesis of CdS quantum dots as barrier layer for increasing dye-sensitized solar cells efficiency, *J. Mater. Sci.: Mater. Electron.*, 2016, 27, 12240–12246.
- 188 W. Zhang, D. Wang, Q. M. Wang and H. Q. Sun, The high performance of quantum dot sensitized solar cells cosensitized with mixed-joint CdS and SnS quantum dots, *ECS J. Solid State Sci. Technol.*, 2019, **8**, Q96–Q100.
- 189 M. Zahedifar, Z. Chamanzadeh and S. M. M. Hosseinpoor, Synthesis of LaVO₄:Dy³⁺ luminescent nanostructured and optimization of its performance as down-converter in dyesensitized solar cells, *J. Lumin.*, 2013, **135**, 66–73.
- 190 J. Roh, S. H. Hwang and J. Jang, Dual-functional CeO₂:Eu³⁺ nanocrystals for performance-enhanced dye-sensitized solar cells, *ACS Appl. Mater. Interfaces*, 2014, **22**, 19825–19832.
- 191 J. Shen, Z. Q. Li, R. Cheng, Q. Luo, Y. D. Luo, Y. W. Chen, X. H. Chen, Z. Sun and S. M. Huang, Eu³⁺-doped NaGdF₄ nanocrystal down-converting layer for efficient dyesensitized solar cells, ACS Appl. Mater. Interfaces, 2014, 6, 17454–17462.
- 192 M. S. Morassaei, A. Salehabadi, A. Akbari, S. H. Tavassoli and M. Salavati-Niasari, Anhanced dye sensitized solar cells efficiency by utilization of an external layer of CaCe₂(MoO₄)₄:Er³⁺/Yb³⁺ nanoparticles, *J. Alloys Compd.*, 2018, **769**, 732–739.
- 193 T. Chen, Y. F. Shang, S. W. Hao, L. Tian, Y. D. Hou and C. H. Yang, Enhancement of dye sensitized solar cell efficiency through introducing concurrent upconversion/downconversion core/shell nanoparticles as spectral converters, *Electrochim. Acta*, 2018, 282, 743–749.
- 194 A. K. Kaliamurthy, H. C. Kang, F. K. Asiam, K. Yoo and J.-J. Lee, Trap-assisted transition energy levels of SrF₂:Pr³⁺-Yb³⁺ nanophosphor in TiO₂ photoanode for luminescence tuning in dye-sensitized photovoltaic cells, *Sol. RRL*, 2021, **10**, 2100411.
- 195 R. Kamal and H. Hafez, Novel down-converting single-phased white light Pr³⁺ doped BaWO₄ nanophosphors material for DSSC applications, *Opt. Mater.*, 2021, **121**, 111646.

- 196 M. Y. Cha, P. M. Da, J. Wang, W. Y. Wang, Z. H. Chen, F. X. Xiu, G. F. Zheng and Z.-S. Wang, Enhancing perovskite solar cell performance by interface engineering using CH₃NH₃PbBr_{0.9}I_{2.1} quantum dots, *J. Am. Chem. Soc.*, 2016, **138**, 8581–8587.
- 197 P. Liu, Y. Sun, S. F. Wang, H. J. Zhang, Y. N. Gong, F. J. Li, Y. F. Shi, Y. X. Du, X. F. Li, S.-S. Guo, Q. D. Tai, C. L. Wang and X.-Z. Zhao, Two dimensional graphitic carbon quantum dots modified perovskite solar cells and photodetectors with high performances, *J. Power Sources*, 2020, 451, 227825.
- 198 Y. Z. Ma, P. Vashishtha, S. B. Shivarudraiah, K. Chen, Y. Liu, J. M. Hodgkiss and J. E. Halpert, A hybrid perovskite solar cell modified with copper indium sulfide nanocrystals to enhance hole transport and moisture stability, *Sol. RRL*, 2017, **1**, 1700078.
- 199 J. J. Ma, G. Yang, M. C. Qin, X. L. Zheng, H. W. Lei, C. Chen, Z. L. Chen, Y. X. Guo, H. W. Han, X. Z. Zhao and G. J. Fang, MgO nanoparticles modified anode for highly efficient SnO2-based planar perovskite solar cells, *Adv. Sci.*, 2017, 4, 1700031.
- 200 S. M. Ali, S. M. Ramay, M. H. Aziz, N. Ur-Rehman, M. S. AlGarawi, S. S. AlGhamd, A. Mahmood, T. S. Alkhuraiji and S. Atiq, Efficiency enhancement of perovskite solar cells by incorporation of CdS quantum dot through fast electron injection, *Org. Electron.*, 2018, 62, 21–25.
- 201 Y. Wang, C. H. Duan, J. S. Li, W. Han, M. Zhao, L. L. Yao, Y. Y. Wang, C. Yan and T. G. Jiu, Performance enhancement of inverted perovskite solar cells based on smooth and compact PC₆₁BM:SnO₂ electron transport layers, ACS Appl. Mater. Interfaces, 2018, 10, 20128–20135.
- 202 T. T. Wu, C. Zhen, J. B. Wu, C. X. Jia, M. Haider, L. Z. Wang, G. Liu and H.-M. Cheng, Chlorine capped SnO₂ quantum-dots modified TiO₂ electron selective layer to enhance the performance of planar perovskite solar cells, *Sci. Bull.*, 2019, 64, 547–552.
- 203 L.-C. Chen, C.-H. Tien, Z.-L. Tseng and J.-H. Ruan, Enhanced efficiency of MAPbI₃ perovskite solar cells with FAPbX₃ perovskite quantum dots, *NanoMaterials*, 2019, **9**, 121.
- 204 X. Y. Zhu, B. Cheng, X. H. Li, J. J. Zhang and L. Y. Zhang, Enhanced efficiency of perovskite solar cells by PbS quantum dot modification, *Appl. Surf. Sci.*, 2019, 487, 32–40
- 205 Y. H. Ma, Y. W. Zhang, H. Y. Zhang, H. Lv, R. Y. Hu, W. Liu, S. L. Wang, M. Jiang, L. Chug, J. Zhang, X. A. Li, R. D. Xia and W. Huang, Effective carrier transport tuning of CuO_x quantum dots hole interfacial layer for high-performance inverted perovskite solar cell, *Appl. Surf. Sci.*, 2021, 547, 149117.
- 206 J. Y. Yin, Y. J. Yuan, J. Ni, J. Y. Guan, X. J. Zhou, Y. Liu, Y. Ding, H. K. Cai and J. J. Zhang, CH₃NH₃PbBr_{3-x}I_x quantum dots enhance bulk crystallization and interface charge transfer for efficient and stable perovskite solar cells, *ACS Appl. Mater. Interfaces*, 2020, **12**, 48861–48873.

Nanoscale Advances

- 207 R. S. Li, Y. F. Dou, Y. S. Liao, D. Wang, G. D. Li, J. H. Wu and Z. Lan, Enhancing efficiency of perovskite solar cells from surface passivation of Co²⁺ doped CuGaO₂ nanocrystals, J. Colloid Interface Sci., 2022, 607, 1280-1286.
- 208 L. Najafi, B. Taheri, B. Martín-García, S. Bellani, D. Girolamo, A. Agresti, R. Oropesa-Nuñez, D. Pescetelli, L. Vesce, E. Calabrò, M. Prato, A. E. D. R. Castillo, A. D. Carlo and F. Bonaccorso, MoS₂ quantum dot/graphene hybrids for advanced interface engineering of a CH3NH3PbI3 perovskite solar cell with an efficiency of over 20%, ACS Nano, 2018, 12, 10736-10754.
- 209 C. Yang, Z. J. Wang, Y. H. Lv, R. H. Yuan, Y. H. Wu and W.-H. Zhang, Colloidal CsCu₅S₃ nanocrystals as an interlayer in high-performance perovskite solar cells with an efficiency of 22.29, Chem. Eng. J., 2021, 406, 126855.
- 210 D. L. Zhou, D. L. Liu, J. J. Jin, X. Chen, W. Xu, Z. Yin, G. C. Pan, D. Y. Li and H. W. Song, Semiconductor plasmon-sensitized broadband upconversion and its enhancement effect on the power conversion efficiency of perovskite solar cells, J. Mater. Chem. A, 2017, 5, 16559-16567.
- 211 J. B. Jia, J. M. Dong, J. M. Lin, Z. Lan, L. Q. Fan and J. H. Wu, Improved photovoltaic performance of perovskite solar utilizing down-conversion NaYF₄:Eu³⁺ nanophosphors, J. Mater. Chem. C, 2019, 7, 937-942.
- 212 W. B. Bi, Y. J. Wu, C. Chen, D. L. Zhou, Z. L. Song, D. Y. Li, G. Y. Chen, Q. L. Dai, Y. S. Zhu and H. W. Song, Dye sensitization and local surface plasmon resonanceenhanced upconversion luminescence for efficient perovskite solar cells, ACS Appl. Mater. Interfaces, 2020, 12, 24737-24746.
- 213 J. Ma, Y. J. Yuan and P. Sun, Approaching 23% silicon heterojunction solar cells with dual-functional SiO_x/MoS₂ quantum dots interface layers, Sol. Energy Mater. Sol. Cells, 2021, 227, 111110.
- 214 A. Thomas, R. Vinayakan and V. V. Ison, An inverted ZnO/ P3HT:PbS bulk-heterojunction hybrid solar cell with a CdSe quantum dot interface buffer layer, RSC Adv., 2020, 10, 16693-16699.
- 215 S. M. Reda, Enhanced efficiency of solar cell using luminescence PbS quantum dots concentrators, J. Fluoresc., 2015, 3, 631-639.
- 216 W. L. Feng, Y. W. Wang, J. Liu and X. B. Yu, Polycrystalline Si nanocorals/CdS quantum dots composited solar cell with efficient light harvesting and surface passivation, Chem. Phys. Lett., 2014, 608, 314-318.
- 217 I. Levchuk, C. Wuerth, F. Krause, A. Osvet, M. Batentschuk, U. Resch-Genger, C. Kolbeck, P. Herre, H. P. Steinruck, W. Peukert and C. J. Brabec, Industrially scalable and cost-effective Mn²⁺ doped Zn_xCd_{1-x}S/ZnS nanocrystals with 70% photoluminescence quantum yield, as efficient down-shifting materials in photovoltaics, Energy Environ. Sci., 2016, 9, 1083-1094.
- 218 M. Jalalah, Y.-H. Ko, F. A. Harraz, M. S. Al-Assiri and I.-G. Park, Enhanced efficiency and current density of solar cells via energy-down-shift having energy-tuning-

- effect of highly UV-light-harvesting Mn2+-doped quantum dots, Nano Energy, 2017, 33, 257-265.
- 219 T. Y. Sun, X. Chen, L. M. Jin, H.-W. Li, B. Chen, B. Fan, B. Moine, X. S. Qiao, X. P. Fan, S.-W. Tsang, S. F. Yu and F. Wang, Broadband Ce(III)-sensitized quantum cutting in core-shell nanoparticles: Mechanistic investigation and photovoltaic application, J. Phys. Chem. Lett., 2017, 20, 5099-5104.
- 220 D. L. Zhou, D. L. Liu, G. C. Pan, X. Chen, D. Y. Li, W. Xu, X. Bai and H. W. Song, Cerium and ytterbium codoped halide perovskite quantum dots: A novel and efficient downconverter for improving the performance of silicon solar cells, Adv. Mater., 2017, 42, 1704149.
- 221 M. Rwaimi, C. G. Bailey, P. J. Shwa, T. M. Mercier, C. Krishnan, T. Rahman, P. G. Lagoudakis, R.-H. Horng, S. A. Boden and M. D. B. Charlton, FAPbBr₃ perovskite quantum dos as a multifunctional luminescentdownshifting passivation layer for GaAs solar cells, Sol. Energy Mater. Sol. Cells, 2022, 234, 111406.
- 222 Y. M. Li, O. S. Zhang, L. Y. Niu, J. Liu and X. F. Zhou, TiO2 nanorod arrays modified with SnO2-Sb2O3 nanoparticles and application in perovskite solar cell, Thin Solid Films, 2017, 621, 6-11.
- 223 M. X. Huang, Z. Z. Lu, L. L. Wen, X. S. Zhang, T. J. Huang, Y. B. Meng, J. J. Tang and L. Y. Zhou, Core/shell-structured TiO2/PbS phoanodes for high-performance CsPbBr₃ perovskite solar cells, Mater. Lett., 2019, 256, 126619.
- 224 Z. H. Wu, Y. Z. Wang, Y. H. Zhang, W. J. Zhang, Q. R. Liu, Q. M. Liu, Q. Chen, Y. L. Li, J. S. Li and D. Y. He, Enhanced performance of polymer solar cells by adding SnO₂ nanoparticles in the photoactive layer, Org. Electron., 2019, 73, 7-12.
- 225 E. J. Lee, D.-H. Kim and D.-K. Hwang, Effect of embedded chalcogenide quantum dots in PbBr2 film on CsPbBr3 inorganic perovskite solar cells, J. Ind. Eng. Chem., 2020, 90, 281-286.
- 226 X. H. Luo, Z. Y. He, R. W. Meng, C. Zhang, M. W. Chen, H. F. Lu and Y. P. Yang, SnS quantum dots with different sizes in active layer for enhancing the performance of perovskite solar cells, Appl. Phys. A, 2021, 127, 317.
- 227 P. Kumnorkaew, N. Rattanawichai, C. Ratanatawanate, S. Yoriya, K. Lohawet, Y. X. Zhao and P. Vas-Umuay, Influence of PbS quantum dots-doped TiO2 nanotubes in TiO2 film as an electron transport layer for enhanced perovskite solar cell, IEEE J. Photovoltaics, 2020, 10, 287-295.
- 228 A. Kirkeminde, R. Scott and S. Q. Ren, All inorganic iron pyrite nano-heterojunction solar cells, Nanoscale, 2012, 4, 7649-7654.
- 229 J. S. Niezgoda, E. Yap, J. D. Keene, J. R. McBride and S. J. Rosenthal, Plasmonic Cu_xIn_yS₂ quantum dots make photovoltaics than their nonplasmonic better counterparts, Nano Lett., 2014, 14, 3262-3269.
- 230 M. A. Najeeb, S. M. Abdullah, F. Aziz, Z. Ahmad, R. A. Shakoor, A. M. A. Mohamed, U. Khalil, W. Swelm, A. A. Al-Ghamdi and K. Sulaiman, A comparative study on the performance of hybrid solar cells containing ZnSTe

QDs in hole transporting layer and photoactive layer, *J. Nanopart. Res.*, 2016, **18**, 384.

- 231 F. Xu, Y. Sun, H. P. Gao, S. Y. Jin, Z. L. Zhang, H. F. Zhang, G. C. Pan, M. Kang, X. Q. Ma and Y. L. Mao, Highperformance perovskite solar cells based on NaCsWO₃@NaYF₄@NaYF₄:Yb,Er upconversion nanoparticles, *ACS Appl. Mater. Interfaces*, 2021, **13**, 2674–2684.
- 232 J. Yu, Y. L. Yang, R. Q. Fan, D. Q. Liu, L. G. Wei, S. Chen, L. Li, B. Yang and W. W. Cao, Enhanced near-infrared to visible upconversion nanoparticles of Ho³⁺-Yb³⁺-F⁻ tridoped TiO2 and its application in dye-sensitized solar cells with 37% improvement in power conversion efficiency, *Inorg. Chem.*, 2014, 53, 8045–8053.
- 233 D. Y. Li, W. F. Sun, L. X. Shao, S. Y. Wu, Z. Huang, X. Jin, Q. Zhang and Q. H. Li, Tailoring solar energy spectrum for efficient organic/inorganic hybrid solar cells by upconversion luminescence nanophosphors, *Electrochim. Acta*, 2015, 182, 416–423.
- 234 N. N. Yao, J. Z. Huang, K. Fu, X. L. Deng, M. Ding, M. H. Shao and X. J. Xu, Enhanced light harvesting of dye-sensitized solar cells with up/down conversion materials, *Electrochim. Acta*, 2015, 154, 273–277.
- 235 N. Chander, A. F. Khan, V. K. Komarala, S. Chawla and V. Dutta, Enhancement of dye sensitized solar cell efficiency via incorporation of upconverting phosphor nanoparticles as a spectral converters, *Prog. Photovoltaics*, 2016, 24, 692–703.
- 236 M. He, X. C. Pang, X. Q. Liu, B. B. Jiang, Y. J. He, H. Snaith and Z. Q. Lin, Monodisperse dual-functional upconversion nanoparticles enabled near-infrared organolead halide perovskite solar cells, *Angew. Chem., Int. Ed.*, 2016, 55, 4280–4284.
- 237 L. Liang, M. Liu, Z. W. Jin, Q. Wang, H. R. Wang, H. Bian, F. Shi and S. Z. Liu, Optical management with nanoparticles for a light conversion efficiency enhancement in inorganic γ-CsPbI₃ solar cells, *Nano Lett.*, 2019, 19, 1796–1804.
- 238 X. S. Lai, X. T. Li, X. D. Lv, Y.-Z. Zheng, F. L. Meng and X. Tao, Broadband dye-sensitized upconversion nanocrystals enable near-infrared planar perovskite solar cells, *J. Power Sources*, 2017, 372, 125–133.
- 239 V. Kumar, A. Pandey, S. K. Swami, O. M. Ntwaeaborwa, H. C. Swart and V. Dutta, Synthesis and characterization of Er³⁺-Yb³⁺ doped ZnO upconversion nanoparticles for solar cell application, *J. Alloys Compd.*, 2018, **766**, 429–435.
- 240 W. J. Shi, Z. L. Zhang, J. Q. Qin, Y. Zhang, Y. Y. Liu, Y. F. Liu, H. P. Gao and Y. L. Mao, Interface modification by upconversion material of Ho³⁺-Yb³⁺-Li⁺ tri-doped TiO₂ to improve the performance of perovskite solar cells, *J. Alloys Compd.*, 2018, 754, 124–130.
- 241 J. W. Liang, H. P. Gao, M. J. Yi, W. J. Shi, Y. F. Liu, Z. L. Zhang and Y. L. Mao, ß-NaYF4:Yb³⁺,Tm³⁺@TiO₂ core/shell nanoparticles incorporated into the mesoporous layer for high efficiency perovskite solar cells, *Electrochim. Acta*, 2018, **261**, 14–22.

- 242 X. S. Deng, C. X. Zhang, J. F. Zheng, X. Zhou, M. D. Yu, X. H. Chen and S. M. Huang, Highly bright Li(Gd,Y) F₄:Yb,Er upconverting nanocrystals incorporated hole transport layer for efficient perovskite solar cells, *Appl. Surf. Sci.*, 2019, **485**, 332–341.
- 243 Q. Y. Guo, J. H. Wu, Y. Q. Yang, X. P. Liu, J. B. Jia, J. Dong, Z. Lan, J. M. Lin, M. L. Huang, Y. L. Wei and Y. F. Huang, High performance perovskite solar cells based on β-NaYF₄:Yb³⁺/Er³⁺/Sc³⁺@NaYF₄ core/shell upconversion nanoparticles, *J. Power Sources*, 2019, 426, 178–187.
- 244 Y. Y. Qin, Z. Q. Hu, B. H. Lim, W. S. Chang, K. K. Chong, P. T. Zhang and H. T. Zhang, So-hydrothermal synthesis of TiO₂:Sm³⁺ nanoparticles and their enhanced photovoltaic properties, J. Alloy, *Comp*, 2016, **686**, 803–809.
- 245 L. J. Wang, W. H. Guo, H. S. Hao, Q. Su, S. S. Jin, H. Li, X. F. Hu, L. Qin, W. Y. Gao and G. S. Liu, Enhancing photovoltaic performance of dye-sensitized solar cells by rare-earth doped oxide of SrAl₂O₄:Eu³⁺, *Mater. Res. Bull.*, 2016, **76**, 459–465.
- 246 A. Pattnaik, S. Jha, M. Tomar, V. Gupta, B. Prasad and S. Mondal, Improving the quantum efficiency of the monocrystalline silicon solar cell using erbium-doped zinc sulphide nanophosphor in downshift layer, *Mater. Res. Express*, 2018, 5, 095014.
- 247 M. S. Pereira, F. A. S. Lima, T. S. Ribeiro, M. R. da Silva, R. Q. Almeida, E. B. Barros and I. F. Vasconcelos, Application of Fe-doped SnO₂ nanoparticles in organic solar cells with enhanced stability, *Opt. Mater.*, 2017, 64, 548–556.
- 248 J. M. Luther, M. Law, Q. Song, C. L. Perkins, M. C. Beard and A. J. Nozik, Structural, optical, and electrical properties of self-assembled films of PbSe nanocrystals treated with 1,2-ethanedithiol, ACS Nano, 2008, 2, 271–280.
- 249 P. R. Brown, D. Kim, R. R. Lunt, N. Zhao, M. G. Bawendi, J. C. Grossman and V. Bulović, Energy level modification in lead sulfide quantum dot thin films through ligand exchange, ACS Nano, 2014, 8, 5863–5872.
- 250 X. S. Lin, D. Y. Cui, X. H. Luo, C. Y. Zhang, Q. F. Han, Y. B. Wang and L. Y. Han, Efficiency progress of inverted perovskite solar cells, *Energy Environ. Sci.*, 2020, **13**, 3823–3847.
- 251 W. Chen, Y. Z. Wu, J. Liu, C. J. Qin, X. D. Yang, A. Islam, Y.-B. Cheng and L. Y. Han, Hybrid interfacial layer leads to solid performance improvement of inverted perovskite solar cells, *Energy Environ. Sci.*, 2015, **8**, 629–640.
- 252 M. A. Haque, A. D. Sheikh, X. W. Guan and T. Wu, Metal oxides as efficient charge transporters in perovskite solar cells, *Adv. Energy Mater.*, 2017, 7, 1602803.
- 253 B. B. Liu, H. Bi, D. M. He, L. Bai, W. Q. Wang, H. K. Yuan, Q. L. Song, P. Y. Su, Z. G. Zang, T. W. Zhou and J. Z. Chen, Interfacial defect passivation and stress release via multi-active-site ligand anchoring enables efficient and stable methylammonium-free perovskite solar cells, ACS Energy Lett., 2021, 6, 2526–2538.
- 254 H. M. A. Javed, M. Sarfaraz, Z. Nisar, A. A. Qureshi, M. Fakhar e Alam, W. X. Que, X. T. Yin, H. S. M. Abd-Rabboh, A. Shahid, M. I. Ahmad and S. Ullah, Plasmonic

dye-sensitized solar cells: Fundamentals, recent

Nanoscale Advances

developments, and future perspectives, *ChemistrySelect*, 2021, **62021**, 9337–9350.

- 255 O. A. Balitskii, Recent Energy Targeted Application of Localized Surface Plasmon Resonance Semiconductor Nanocrystals: A Mini-Review, *Mater. Today Energy*, 2021, 20, 100629.
- 256 B. S. Richards, Enhancing the performance of silicon solar cells via the application of passive luminescence conversion layers, *Sol. Energy Mater. Sol. Cells*, 2006, 90, 2329–2337.
- 257 A. H. G. Niaki, A. M. Bakhshayesh and M. R. Mohammadi, Double-layer dye-sensitized solar cells based on Zn-doped ${\rm TiO_2}$ transparent and light scattering layers: Improving electron injection and light scattering effect, *Sol. Energy*, 2014, **103**, 210–222.
- 258 W. An, J. R. Wu, T. Zhu and Q. Z. Zhu, Experimental investigation of a concentrating PV/T collector with Cu₉S₅ nanofluid spectral splitting filter, *Appl. Energy*, 2016, **184**, 197–206.
- 259 I. Zarma, M. Ahmed and S. Ookawara, Enhancing the performance of concentrator photovoltaic systems using nanoparticle-phase change material heat sinks, *Energy Convers. Manage.*, 2019, **179**, 229–242.

- 260 Z. K. Liu, Y. X. Zhong, I. Shafei, R. Borman, S. Jeong, J. Chen, Y. Losovyj, X. F. Gao, N. Li, Y. P. Du, E. Sarnello, T. Li, W. L. Ma and X. C. Ye, Tuning infrared plasmon resonances in doped metal-oxide nanocrystals through cation-exchange reactions, *Nat. Commun.*, 2019, 10, 1394.
- 261 M. G. Gong, D. Ewing, M. Casper, A. Stramel, A. Elliot and J. Z. Wu, Controllable synthesis of monodispersed Fe_{1-x}S₂ nanocrystals for high-performance optoelectronic devices, *ACS Appl. Mater. Interfaces*, 2019, **11**, 19286–19293.
- 262 C. Beynis, Indium insertions in non-stoichiometric copper sulfides, Cu_xS, and their effect on the localized surface plasmon resonance of the nanocrystals, *Appl. Phys. A*, 2019, **125**, 310.
- 263 A. Verma and S. K. Sharma, Down-conversion from Er³⁺-Yb³⁺ codoped CaMoO₄ phosphor: A spectral conversion to improve solar cell efficiency, *Ceram. Int.*, 2017, 43, 8879–8885
- 264 Y. Q. Yin, M. Q. Wang, V. Malgras and Y. Yamauchi, Stable and efficient Tin-based perovskite solar cell via semiconducting-insulating structure, ACS Appl. Energy Mater., 2020, 3, 10447–10452.
- 265 Y. X. Ye, Y. Q. Yin, Y. Chen, S. Li, L. Li and Y. Yamauchi, Metal-organic framework materials in perovskite solar cells: Recent advancements and perspectives, *Small*, 2023, 19, 2208119.